AN ABSTRACT OF THE DISSERTATION OF

Eric Martin Kratzer for the degree of Doctor of Philosophy in Molecular and Cellular Biology presented on December 3, 2007

Characterization of Acid Sensing Ion Channel (ASIC) in Mouse Olfactory Bulb

Abstract Approved:

_____

Roger P. Simon, M.D.

This study examined the role of acid- sensing ion channels (ASICs) in interneuron synaptic modulation. ASICS are ultra fine discriminators of acidic conditions in the neuronal microenvironment. Each ASIC subunit isoform has innate, subtly different electrophysiological properties and tissue distributions. Structurally, ASICs may form homo- or heteromeric channels, yielding combinatorial functional properties regarding their sensitivity to the extracellular environment, saturation limits, inactivation profiles, and putative roles in the initiation of neuronal injury. Electrophysiology provides direct biophysical monitoring of channel activity and allows pharmacological isolation and manipulation. Fura-2 imaging allows direct visualization of calcium ion flux into neurons, verifying their calcium gating ability. Molecular verification of ASIC protein composition via western blotting and Immunocytochemistry showed anatomical distribution patterns of ASIC isoform combinations in the mouse olfactory bulb (OFB) tissue, the first documentation. Genetic knockout animals also verified results and internal controls were also utilized. ASIC isoforms combine their functions perform environmental sensing, and modulation of synaptic transmissions during normal and pathological conditions.

Characterization of Acid Sensing Ion Channel (ASIC) in Mouse Olfactory Bulb

by
Eric Martin Kratzer

A DISSERTATION

submitted to

Oregon State University

In partial fulfillment of
the requirements for the
degree of

Doctor of Philosophy

Presented December 3, 2007
Commencement June 2008

Doctor of Philosophy dissertation of Eric Martin Kratzer
presented December 3, 2007.

APPROVED:

Major Professor, representing Molecular and Cellular Biology

Director of the Molecular and Cellular Biology Program

Dean of the Graduate School

I understand that my dissertation will become part of the permanent collection of Oregon State University libraries. My signature below authorizes release of my dissertation to any reader upon request.

Eric Martin Kratzer, Author

ACKNOWLEDGEMENTS

This author wishes to acknowledge the Robert Stone Dow Neurobiology Institute for sponsoring my doctoral studies with reliable employment, in particular Roger P. Simon, MD, for enabling my schooling to be completed through his sponsorship.

Dr. ZhiGhang Xiong, Dr. Minghua Li , and Dr. Xiangping Chu assisted with my training in electrophysiology, and all assisted with technical problems and data interpretation. Dr. Jing Quan Lan assisted with tissue histological preparation.

To the Molecular and Cellular Biology Program of Oregon State University.

To OSU Housing and Dining Services for the allowing me to become the first ever graduate student to participate in the Faculty-in-Residence program.

I wish to express my profound gratitude to my PhD committee and my mentors here at Legacy Neurobiology who have fostered my self-determination and enabled me to achieve my personal goal as a scientist.

My most humble and sincere thanks to all.

TABLE OF CONTENTS

LIST OF FIGURES

LIST OF FIGURES (Continued)

DEDICATION

This author wishes to honor Dennis Bray, co-author of the CELL textbook series, whose publication "Protein molecules as computational elements in living cells" (Nature Vol. 376 pp. 307-312 July 27, 1995) made an enormous impact on the evolution of my personal scientific worldview regarding protein function.

This author also wishes to thank my family and friends who always supported my goal of attaining a doctoral degree in molecular and cellular biology.

Characterization of Acid Sensing Ion Channel (ASIC) in Mouse Olfactory Bulb

Chapter One: Introduction

This dissertation outlines work performed using the olfactory bulb brain region of the mouse. The biochemical presence and the biophysical activity of acid sensing ion channel (ASIC) protein was experimentally confirmed by the techniques of electrophysiology, calcium imaging, western blotting, immunocytochemistry (ICC), and perhaps conclusively, the use of genetic knockout animals for verification of the above studies. This work confirms the heteromeric composition of ASICs in the mouse OFB.

During the completion of this dissertation, an interesting crystallographic study proposed a channel composition of three subunits. However, no work has ever definitively shown the number of functional ASIC subunits *in vivo*, or examined whether this number might vary; the interchange or removal or addition of subunits is suggested here to correspond with functionally desensitized state, at least under the extreme conditions required for the aforementioned study. This timely coincidence of structural and functional discoveries will be elaborated upon in the discussion chapter.

Intro: ASICs are expressed in the brain

The superfamily of sodium channel members include the amiloride-blockable epithelial sodium channel (ENaC), the (nematode) C. elegans' mechano-sensing Degenerins (DEG), and a (molluscan) FMRFamide-gated channel (FaNaC) as well as other (known: DRASICs, and unknown: see below) permutations of this sodium channel's signaling mechanism[1]. Utilization of a human brain cDNA library has revealed yet another sub-family of sodium channels, termed BNaC1 and BNaC2, which are phylogenetically distinct and equally divergent from other members of the DEG/ENaC superfamily[1]. Mouse brain samples were used for Northern Blot analysis and *in situ* hybridization experiments, which confirmed that both BNaC1 and BNaC2 genes are expressed in nearly all brain neurons, but with varying patterns (ratios) of co-expression[1]. In a similar fashion as their ASIC counterparts, these BNaC subunits likely form channels together, although that does not exclude the possibility that they participate in human brain functions in a manner similar to ASICs[1].

Evolutionary origin of ASICs

The evolutionary context of this ion channel should illuminate ASIC's role in the physiology of organisms other than humans, or even mammals. A very distantly related (~420 million years divergent from mammals) toadfish species (*Opsanus tau*) underwent a complete protein sequence comparison revealed a 76% identity with the (ASIC equivalent) rat orthologue[2]. Regarding sequence homology, the most conserved regions of the protein were the second transmembrane domain, and the ectodomain, whereas the least conserved regions were the first transmembrane domain and both of the protein's free ends; the amino and carboxy termini [75]. The most important functional difference between the rat and fish (ASIC) channel biophysical properties is the 25-fold faster rate of desensitization (for the fish channel), which is functionally performed by a three-residue cluster within the extracellular domain of the fish channel[2]. The fish ASIC half-maximal activation of pHo 5.6 differs significantly from mammalian ASICs[2]. Please recall

those mammalian values are: ASIC1a: 5.8, ASIC2a: 4.5, ASIC 1a+2a: 5.5. The relevance of this evolutionary divergence of environmental (pH) sensing parameters makes sense when, as the ocean environment is slightly alkaline, almost exactly pH 7.3.

Olfaction is direct environmental chemical sampling

Sensory modalities transmit the intent of the signal being conveyed, and often these signals must first be transduced into chemical or electrical impulses that the mammalian brain may integrate and interpret. Of all sensory modalities, olfactory sensation, the act of smell, is the most direct and forthright in mechanism. The smell perceived is the chemical itself, not a representation of the chemical; visual images are surface refractions, auditory sounds are vibrations transduced into electrical signals, whereas the sense of smell is just the raw input of the chemical directly into the sensory system; in effect the sense of smell is a direct chemical sampling of the environment.

Amplification and discrimination function of the OFB

The stereochemical attachment requirements for molecular recognition and (ligand) binding are the same for odorant as they are for other chemical signals and neurotransmitters; the receptor's energy-minima (electron) field forms a cooperative "best fit" (quantum mechanical) with the three-dimensional valence volume of the ligand[3]. The physiological ability of the olfaction system to detect and discriminate between thousands, if not hundreds of thousands of distinct odorant molecules is housed in the molecular diversity of the receptors, the anatomical distribution of them, and their interactive, overlapping receptive fields that allow for amplification via summation, cancellation via subtraction, and single odorant signal specificity. The inherent mixture of chemicals that form the basis of the olfaction sensory modality requires that the olfaction system of identification not only recognizes each chemical component of the mixture, but also the ratios/percentages of each and how they interact with each other, often in a ratio

dependent manner; thus, the end result cannot be predicted from the known sample composition, given the combinatorial complexity[4].

Sensory field overlap requires heteromeric functions

Recalling the vertebrate organism-developmental context of overlapping zones of hormonal influence/ gene induction, the notion of combinatorial chemical influence empowering gene expression changes is valid and applies to the theme herein of overlapping functional signal inputs that, by their overlap, create and define new, additional signals. The combinatorial 'receptor code' scheme entails that each odorant is recognized by a set of receptors, and that many receptors are capable of recognizing (re: binding) several different odorants; which are likely to be very structurally similar. There are many receptors types that are distributed throughout the olfactory epithelium, and the summation of their inputs are integrated into a set of axonal transmissions that terminate in the 'smell' integration center called the entorhinal cortex; bypassing the thalamus entirely. It should be noted that olfaction is the one sensory modality that is not signal-routed through the thalamus; so it is singular in that regard. The receptor field of the olfaction system is an integrated network capable of detection, discrimination, and amplification of any given olfactory signal; the modulation and transmission of these signal "intentions" are carried /transduced through several cell types before their action potentials finally arrive at the brain's entorhinal cortex. The physiological pattern of neuronal activation resultant from olfaction is distinct for each "smell" and has overlapping zones of activity, as well as multiple activation and cancellation mechanisms inherent to the chemical constituents themselves; so all individual components *and* combinations of odorants are important in the activation of the olfaction system[5].

OFB Interneurons

The generation of axonal current is not the only function of nervous tissue; the role of inter-neurons in the normal synaptic transmission process is not very well

understood. Great interest in the role of inter-neurons in the modulation of acute injury and chronic disease states and their putative usefulness as possible therapeutic interventions has thrust the once shadowed inter-neuron into the neuroscience metaphorical “microscope”. Overlapping functional zones of responsibility for the evaluation of a discriminatory response is a common characteristic in sensory modalities. The interlacing network of cellular subtypes in the olfactory system are electrochemically linked and physical connected via gap junctions as well, providing the ideal structure cellular arrangement for the modulation of sensory input; the extracellular generation of global influencing (electrical) current concurrently with the rapid and regulated diffusion, the so-called “resource sharing” of intracellular components and diffusible signaling elements. Mitral and tufted cells contribute to a large overall percentage of the olfactory bulb cellular population, among other inter-neuron subtypes, the final summations of sensory inputs are to be further routed to the entorhinal cortex, where the “smell” perceptions will be integrated with memory engrams of previous experiences and the entailed biases and preferences relevant to survival will be consciously experienced a few milliseconds later.

ASIC context, biophysics, pharmacology

The synaptic cleft is an acidic microenvironment; the release of neurotransmitters from synaptic vesicles indeed alters the pH locally and transiently; the reaction-volume and time-duration of these pH changes are parameters of action that are monitored by the cell through several molecular mechanisms, one of which is the ASIC protein[6]. Characterization of amiloride sensitivity found in some sodium channels in effect delimited a new protein class; that of the external sodium channel degenerin ion channel, the ENaC-Degen family[7]. The near-ubiquitous distribution of ENaC-Degen channels in tissues of both vertebrate and invertebrates directly implies a diverse array of functions; from conducting simple ion exchange to maintain homeostasis, to providing regulation of neuronal function and synaptic transmission via (neurotransmitter) receptor functionality[7].

ASIC1 protein is expressed at a near-constant level during embryonic (brain) development from embryonic day 12 well into postnatal adolescence[8]. This study confirms the presence and activity of ASICs in (neonatally derived) primary cultures through their *in vitro* development, and also in adult animal samples. The expression pattern and tissue distribution of ASIC 1 isoform was determined by immunocytochemical staining with specific antibodies; CNS locations included the hippocampus, the cerebellum, and the cerebral cortex[8]. This study confirms ASIC isoforms 1a and 2a localized in the mouse olfactory bulb.

Tissue distribution and role ASICs

Localization of ASIC1a to dendritic spines in organotypic cultures (tissue slices) of brain hippocampus verified the assertion of pH monitoring and has been re-verified in other brain regions by several laboratories[6]. ASIC1 has a direct correlation on the density of dendritic spines located on the postsynaptic (excitatory) side of the cleft (the volume for neurotransmitter release); any increase in ASICs lead concomitantly to spine number increases[6]. The precise mechanism of ASIC modulation of spine density involves well-known participant in cellular regulation; the Ca(2+)-mediated, Ca(2+)-Calmodulin-dependent protein kinase II (CaMKII); ASIC1a protein levels mirrored phosphorylation changes in this enzyme, and conversely, inhibition of CAMKII prevented sine density adjustment by ASIC1a[6]. The cellular localization within individual neurons was also determined via immunostaining, with channels being present all over the cell body (soma) and also extensively covering both dendritic and axonal projections[8]. This study also confirmed the localization of ASICs with certainty on the cell body, and with somewhat less clarity for all other projections (axons and dendrites). Perhaps by design, ASIC1 was not found in the subcellular locations that have dramatic changes in pH on a routine basis; the synaptic cleft and the associated membranes and vesicles, all of which are so-called microdomains that reach very low pH values, based on the neurotransmitters they contain and release[8].

ASIC biophysical properties are modulated by ASIC2

The preference of ASIC protein for various ions proceeds form most to least favorable: sodium (Na^+), calcium (Ca^{2+}), then potassium (K^+), with the primary activation-triggering ligand to be protons (H+), or perhaps hydronium ions (H_3O^+)[9]. The uncomplicated structure of this channel implies a simple, straightforward physiological function[9],[10]. The transient activation status of the ASIC channel directly indicates a rapid on/off ligand binding affinity, as well as a likely conformational (shape-change) to adjust the channel's biophysical parameters[9]. Several studies conflicted before this issue was resolved to indeed be an allosteric, conformational change mechanism of ASIC gating[11],[12] ,[10].

The rapidity of extracellular acidification during pathologies in the nervous system occurs both locally and globally, when entire brain regions become quickly starved of their otherwise constitutive oxygen and glucose supplies, notably during episodes of ischemic insult (stroke) or during traumatic brain injury[9]. The functional task of sensing ion concentration, in particular protons (pH) is a molecular mechanism directly related and suited for the early warning systems of pain reception (nociception) and the immediacy of gustatory functions (taste)[9]. Both of these sensory modalities requires an extremely rapid identification of the 'signal' and recognition of the signal as good/bad, something to be swallowed (delicious) or perhaps spat -out (dangerous). This rapidity of function also applies to the sensory modality of smell.

An extremely unusual biochemical mechanism, perhaps a unique one thus far discovered, is responsible for the inhibition-mechanism; the channel's affinity for protons is actually altered by the binding of the protons (H^+) themselves (likely as hydronium ions H_3O^+)[13]. This autofeedback loop is initiated by the (proton triggered) relatively small increase in the sensitivity of the channels to (normal or pathological) albeit subtle changes in the environmental hydrogen ion concentration (pH), which forces the channel into a desensitized state[13].

The biophysical traits that best exemplify the ASIC1a protein are it's triggered opening by ligand-binding of protons (and protonated water) and the extremely rapid parameter called desensitization, which defines how rapidly the channel is turned off by an 'overflow' of signal (cation inflow)[2]. Desensitization rate is a major indicator of cellular function; as this parameter defines the threshold of operation for the channel; any more (proton) concentration and the protein can no longer operate its function of molecular recognition; any further incoming information signal is simply not 'sensed' by the channel. The so-called secondary characteristics of ASICs, the biophysical parameters that modulate the actual raw (primary) function (of channels gating) include the ability to shift the pH sensitivity to the channel's maximum threshold, and subsequently the time-durations of recovery required following over-stimulation (desensitization recovery rate)[14]. Administration of constituent ASIC1a blockade to establish a state of chronic ASIC desensitization is being investigated as a possible strategy for therapeutic intervention in the early onset stages of acute ischemic episodes like stroke and aneurysm[13].

Detection of the ASIC-null heterozygotic alleles allowed segregation of the cellular populations, and a null strain of the mutated neurons to be cultured for *in vitro* verification of individual contributions of ASIC isoforms[15]. Directly verified by electrophysiology, the current amplitude of the heteromeric channels correlated proportionally with both the "collaborative" participation of each subunit, as well as the overall total (absolute) ASIC population-contribution[15]. The proton-gated current that characterize ASICs are directly proportional to each contributing member of the tertiary (protein) structure, the combination of isoforms specifically defines the functional parameters of the neuron's physiology[15]. ASIC1a was the determining contributor of the current amplitude in this hippocampal *in vitro* study of null populations[15]. ASIC1a is the subunit that allows direct cation flow inward, generating the current summations required for synaptic transmission[15].

The ASIC2a isoform/subunit serves as a modulating influence on channel function. The biophysical parameters that characterize the channel (beyond its characteristic ion flux) include external ligand sensitivity with concurrent adjustment (recovery), the desensitization of the channel caused by excess signal and that subsequent recovery, and finally, some influence to the effects of pharmacological modulators, such as oxidation-reduction agents, quinine, glucose, or other specific drugs[16],[15],[17]. To summarize, the ASIC2a subunit had little effect on amplitude, but influenced desensitization, recovery from desensitization, pH-sensitivity, and the response to modulatory agents.

ASIC biophysical (secondary) parameters other than (primary) current amplitude were also affected by the application of acidification or alkalinization; proton dose-response curves were shifted to a less acidic pH value, while the steady-state inactivation curve was altered to a more acidic pH value when the pH(i) was experimentally increased (more alkaline)[14]. A pronounced increase in the rate of ASIC desensitization recovery was shown to be an effect of the internal cellular alkalinization[14]. Altering pH(i) also triggers changes in the calcium internal distribution (from mitochondrial stores), likely through MAPK pathways, and a general membrane depolarization, which can have profound and long-lasting cellular consequences[14]. Presumably the internal pH is monitored and regulated just as the external inward ion flow is regulated; so the importance of ASIC protein as a fundamental biological mechanism as a proteinaceous sensor, and it's putative role in acidosis-mediated neuronal pathologies should not be underestimated.

Heteromeric channels

Heterogeneous populations of ion channels display a combinatorial scheme of their various parameters, as they are in effect combining their pharmacological roles through the physical cooperation of subunits; each of which has distinct properties unto themselves[18].

Comparison of ASIC2a with ASIC2b (an N-terminal splice variant of ASIC 2a) using a wide array of molecular biological tools, including cDNA library screening, RT-PCR analysis, and immunohistochemical staining, supports the notion of functional heteromeric assemblies of (different) ASIC isoforms[19]. RT-PCR analyses of rat taste bud cellular extracts provided evidence for the presence of ASIC2a & 2b transcripts, and was confirmed by *in situ* hybridization[20]. Biochemical immunoprecipitation studies using of cell extracts using bead-columns, and immunohistochemistry on tissue samples, each directly detected (via antibody binding) all of these ASIC subunits (2a & 2b), as well as heteromeric complexes of these ASIC isoforms[21]. This strongly suggests that this theme of combinatorial isoform expansion of functionality is perhaps a ubiquitous physiological mechanism of both the CNS and PNS.

Isoform combinations generate biological functions

Verification of the heterologous expression (in the DRG) conjoined with their combinatorial subunit (isoform) functional cooperation by the family members of (DEG/ENaC) channel subunits; ASIC, BNC1, and DRASIC; targeted gene (mutational) disruptions of each (of these three channels types) confirmed (by non-abolished current analysis) the extensive cellular utilization of hetero-multi-merization of the (isoform combinations) to functionally expand the ranges of sensing, gating, modulating, regulating, and other parameters of channel function enhancing organism survival and procreation[22]. Recapitulation of the argument above generally says that protein subunits may be interchanged in a variety of structural arrangements to provide a functional expansion of cellular capabilities;

the combinatorial chemistry industry methods, only this process has evolved by cellular needs and selections for eons untold[22].

Heteromeric channels, by their construction and inherent activity, form complexes with functionally expanded abilities, becoming more than the sum of their subunits through the principle of (biological) synergy. New functional combinations of subunits provide the heteromeric channel with novel properties unavailable to the single isoform constituent brethren of homomeric channels[23].

Heteromeric channels, combined with uncharacterized post-translational modifications add another level of discrimination capability to the channel population. Being able to ascertain what actually is a signal and what is not defines the sensitivity of the signal receptor system (ligand-based or otherwise), while the discrimination is detecting the differences between two non-identical signals that may be very similar.

The individual properties are known, but the range of possible modifications to these individual protein isoforms is not known. Determination of the extent of contribution by non-genetic based modifications is currently probably beyond the reach of molecular methods. Some clarification of these matters can be expected in the near future given that ASICs genes are available for genetic transfection into model organisms such as Xenopus eggs and various host cell lines. However, the species- and tissue-specific protein machinery and covalent modifications that regulate ASIC function will not always be present in such systems. The resultant observations will of course be informative in the sense that they are functioning channels operating normally, but they will reflect the lack of what may ultimately turn out to be an important ‘supporting’ *in situ* proteinaceous framework that is dedicated to the movement and functional modulation of these channels.

Immunoprecipitation studies only confirm the possibility/ ability for two proteins to associate covalently (bind together); this is not a direct indication of their association *in vivo,* nor should it be construed as such. ASIC association with another mammalian degenerin, MDEG, was demonstrated by their co-precipitation together, but as alluded to above, this does not directly implicate a functional relationship *in vivo*. When these two proteins were expressed in the model-organism system of the oocytes, the electrophysiological properties measured were indeed novel, and essentially combinations of the biophysical parameters (pH sensitivity, kinetics, and ion selection) of both protein sub-classes[23]. This clearly illustrates that ASICs and MDEGS may form (isoform) (heteromeric) complexes that expand the diversity of human brain physiology, as their application in 'sensing' functions likely included combinations with biophysical sensing "overlap", allows the full physiological pH range to be continuously monitored[23]. The modulation role of subunit MDEG2 functions to embed with and alter the ion kinetics of known channels, but is insensitive to mutations that cause neuro-degeneration, and is notably not activated by lowering the pH[24]. Different combinations entail altered parameters of pH sensitivity, ion selectivity, and kinetic responses[24]. The biphasic current produced by these heteromeric channels are poor gatekeepers; they do not distinguish between sodium and potassium very well, leading to a prolonged current that is indicative of the physiological sensation of acid-induced pain[24].

Chapter Two: Literature Review

ASICs relevance to neuronal pathology

Ischemia produces acidosis conditions, lowering the micro-environmental pH surrounding the neurons expressing ASICs; which in turn are triggered by the increased proton concentrations (a pH decrease) produced by various pathological conditions, as well as normal conditions of excitatory neurotransmitter release in the synaptic cleft, which spill acidic (neurotransmitter) contents[25]. ASIC current activation directly leads to membrane depolarization[25]. ASICs permeable to calcium become nonselective, allowing both sodium and calcium ions to flow inward, contributing to the generation of current[25].

The chronic pH changes associated with long-term pathologies such as ischemia and seizure activity promote changes in the current-responses and cellular distribution of the ASIC (and other) 'sensor' proteins[6]. Clearly a pH monitoring system operates on the cellular level, functioning as a 'sensor' of many related chemical interaction; pH changes and oxidation-reduction reaction-conditions are assayed by the mammalian nervous system (CNS and PNS)[6]. The importance of clinical application derived from fundamental scientific research is not to be understated. ASICs are clearly a cellular "early warning system" that triggers a cascade of protective events, as well as being the threshold-trigger for actual cell-death, should the brain injury be so severe. Pharmacological blockade of ASIC1a, and genetic removal of ASIC1a (gene knockout) both result in a remarkable level of protection to brain tissue in the surrounding zones of injury[25,13]. The time window of ASIC- designed interventions, most notably the spider toxin PcTX, is well over three hours (!)[25].

A common mechanism for both spreading depression and ischemia would rely on ion channel permeability changes resulting in ion influx of both sodium and calcium[26]. Tissue damage triggered by acidosis, oxygen-glucose deprivation, or

other ischemic insults calcium-entry occur via a pathway that is separate and distinct from the glutamate receptor system; a receptor / ion channel that is able to conduct calcium under pathological conditions, the acid-sensing ion channels (ASICs)[27]. The toxicity of intracellular calcium levels are not well understood; apparently there exists a cellular threshold of acceptable or useful calcium concentration, beyond which toxic damage may be unavoidable[28]. Clinical therapies relevant to brain injury are experimentally derived from the molecular utility of their neuro-chemical interaction; the acid sensing ion channel isoform 1a (ASIC 1a) is the most promising target for a potential stroke / brain ischemia treatment because it directly gates and influxes calcium, the primary determinant of the extent of neuronal injury[16],[29],[10],[30]. Confirmation of ASIC 1a involvement in this form of glutamate-independent, acidosis mediated system of ion compensation and reduction of neuronal injury is available from several laboratories[16],[10],[30].

The role of ASICs in brain ischemia is being uncovered incrementally, with new discoveries underscoring this endogenous ion channel/ receptor system as a means to further develop novel therapeutic treatments based on cellular chemistry[27]. The role of mediating calcium entry has been attributed to ASICs for several reasons; first, ASIC knockout mice are impervious to the same level of acidosis-type damage that severely injures their native brethren[27]. Second, transfection of ASIC genes into Chinese hamster ovary cells (CHO cells), or HEK-293 cell line, or even Xenopus oocytes will incorporate the ASIC gene products into the cellular membranes, and establish the same (ASIC) sensitivity to acidification and oxidative stress, along with the concomitant calcium entry and damage increase[27]. Additionally, ASICs have been demonstrated to gate calcium as confirmed by fura-2 imaging[31].

Ischemic injury models have been advanced to explain the roles of acidosis and NMDA excitatory cascades in the tolerance towards and mediation of ischemic insult[32]. Several interacting biochemical pathways are responsible for the complex behavior and pathology of cerebral ischemia; a commonality of these pathways is

the pervasive event of acidosis. The precise targets of free radical attack are not known; presumably they react with the nearest possible oxidative component available. The chemistry of these reactions is immediate and nonspecific[33].

> "Enhanced acidosis may exaggerate ischemic damage by one of three mechanisms: (i) accelerating free radical production via H(+)-dependent reactions, some of which are catalyzed by iron released from protein bindings by a lowering of pH, (ii) by perturbing the intracellular signal transduction pathway, leading to changes in gene expression or protein synthesis, or (iii) by activating endonucleases which cause DNA fragmentation."[33].

Pre-treatment of cultured hippocampal cells with mild to moderate acidosis (pH 6.6) was able to block the inward calcium currents that normally follow such exposure[32]. This effect has been studied in greater detail since then, and the application of this observed phenomenon in cultured cells has lead to the expansion of *in vivo* treatments that mediate ischemic damage under the appropriate "pre-conditions"[32]. Cultured mouse cortical cells exposed to toxic levels of oxidative stress via application of hydrogen peroxide were statistically more damaged as a population (that is, the injury was potentiated) with concurrent treatment of acidosis conditions equating to a physiological pH of 6.2[34]. The compensatory antioxidant capacity of the culture was assayed through monitoring the biochemical activity of several key enzymes; acidosis conditions markedly reduced by 50-60% ($p < 0.001$) the activity of glutathione peroxidase and glutathione S-transferase[34]. Targeting a specific cellular antioxidant enzyme, mercaptosuccinate, also produced increases in culture injury during the aforementioned hydrogen peroxide trials[34].

Further support for the involvement of oxidative stress in neuropathology comes from the use of iron chelators in an attempt to ameliorate the exacerbated injury caused from the combination of acidosis and oxidatively injurious physiological states. The two very structurally different iron chelators, desferrioxamine and N,N,N',N'-tetrakis (2-pyridylmethyl) ethylenediamine (aka TPEN), under pH 7.2

and pH 6.2 conditions, both significantly reduced hydrogen peroxide-induced neuronal death[34]. These chelator-studies are unable to distinguish the oxidative injury resultant from possible impaired enzymes that normally mediate antioxidant functions, from the obvious increases in intracellular iron levels that the chelators themselves target, and in effect, assay[34].

However, when taken together, the combination of oxidative stress, acidosis, and other stressors like glucose deprivation that occur during ischemic conditions produces a self-sustaining injurious-state within individual cells, that given their interconnectedness, expands the overall (brain) tissue damage[34].

CNS expression of ASIC protein directly and fundamentally contributes to synaptic plasticity through the modulation of divalent cation (ions with a two positive charge) flow, altering the individual cell's current and it's subsequent signaling to other cells. Since ASICs normally allow sodium ion (Na^{+2}) flow, they participate in basal level cellular (current flow) activity. ASICs are non-voltage gated ion channels, unaffected by the continuously altering electrical milieu of the neuron's microenvironment. ASICs provide a pathway for other divalent cations to enter the cell, albeit at different rates and concentrations. Zinc and calcium are two important divalent cations with cellular roles whose very different effects are critically dependent upon their release context (local microenvironmental concentration increase). ASICs are a system to detect these changes.

Calcium is a well-understood cellular participant in processes intimately linked to cell signaling and outright survival. The gating of calcium by ASICs under the proper conditions is the basis for their modulation of neural activity. Elevating the cytosolic calcium level can produce a wide range of effects, some beneficial, some deleterious; depending critically on the cellular context of the calcium release. If the calcium influx exceeds the cellular threshold and triggers the additional release

of mitochondrial calcium stores, that would establish difficult survival circumstances for the neuron[35].

The deleterious effects of cerebral ischemia may be simulated *in vitro*, and these cultures may be damage-assayed under pathological conditions by measuring disgorged substances during the death-process. Many critical enzymes and other cellular metabolites are part of this dumping of cellular volume as the cytoskeletal framework disassembles during necrosis onset.

Ischemia

The locus (initial site/origin) of a mammalian brain injury is surrounded by a tissue-dependent zone of secondary injury called the penumbra, where blood flow impairment, if not restored, will trigger cell death in a few hours[36]. The tissue zone borders of secondary brain injury are strongly determined by inflammation that occurs during and after injury events, which is specifically guided by pro-inflammatory molecules[37]. Interruption of critical metabolic pathways like glycolysis by using 2-deoxyglucose as a non-reactive precursor, or by using potassium cyanide (KCN) to directly prevent oxidative phosphorylation are chemical treatments that mimic ischemic conditions in animal models[38].

Proposed mitochondrial mechanisms of surging calcium require that the inner membrane of the cristae be depolarized to allow free permeability of the internal mitochondrial calcium stores[39]. Free radical attack on mitochondria results in a breakdown of the partitioning of the mitochondrial wall, allowing ion contents to spill uncontrollably[33]. Mitochondrial failure is the threshold mark for the demarcation of moderate (recoverable) injury between severe (not recoverable, death) injury manifestations of the ischemic process[39]. Essentially, once the neuron’s internal ion regulatory system is lost, the cell is doomed. Experimental data clearly supports the (ischemic) model that mitochondrial failure occurs, but no definitive causal connection has been unambiguously established through

experimental procedures such as calcium-45 loading, or assays that directly indicate a decline in metabolic energy production [15]. Internal cellular calcium levels are monitored by the aqueous soluble factors that continually assay concentrations of the cell's chemical constituency[39].

Pharmacological blockade of voltage-gated sodium channels by tetrodotoxin produced protective effects when given up to 30 minutes post-injury [16]. The direct interaction of this toxin with an ion channel, and the subsequent reduction in overall ischemic damage, indicates a role for voltage dependent sodium channels in the process of recovery of function following brain damage.

Reperfusion dangers

Ischemic damage leads unwanted mitochondrial discharge of several key enzymes, such as nitric oxide synthases and xanthine oxidases, among others[40]. The superoxide cascade is a regrettable circumstance of the rapidity of oxygen re-perfusion following ischemic insult. In addition to being extremely reactive species themselves, nitric oxide and superoxide are likely to form the peroxynitrite ion, which is very toxic via the deleterious modification of DNA, along with the induction of necrotic and apoptotic pathways[40].

Preconditioning

The phenomenon of preconditioning has been outlined experimentally as an administration of a short-term sub-lethal ischemic insult, followed by several days of recovery, which in effect provides neuroprotection via an unknown set of mechanisms, culminating with the researcher sacrificing the animal and studying these aspects of neuronal degeneration and possible rescue in more detail at the cellular level[41]. Gene up-regulation resultant from injurious states of ischemia showed virtually no overlap with those genes altered by the ischemic pre-conditioning phenomenon[42]. Selective subunit modulation or sequestration allows the cell to direct functional changes to sub-groups of receptor complexes, that in

turn will functionally expand the range/ concentration threshold of detection for certain deleterious molecules or in effect alter the parameters of the signal transduction chain of causal molecular events required for the prevention of further damage, or rather, the untoward spreading of said damage. The duration and severity of initial injury are factors determining the cellular pathway of death to be chosen by the cell; the result will either be the controlled, regulated process of apoptosis, or the uncontrolled chemical cascade of necrosis. The precise locus of injury is termed the ischemic core, with the surrounding tissue comprising the penumbral region, which is sensitive to the release of toxins attributed to the cellular death process[43].

NO and cellular context

The context-dependent role of nitric oxide (NO) in ischemic brain injury entails that the free radical NO may be alternately a neurotoxin or a signaling molecule[44]. NO has been implicated in the mechanisms of brain ischemia, in that genetic mutant knockouts of nitric oxide synthase (NOS) have been utilized to further understand the role of reactive oxygen species in these pathologies[44]. That neuroprotective or exceedingly toxic effects of nitric oxide (NO) are critically dependent upon the cellular conditions and through what molecular pathway NO is released from. Even more important is the precise time during the development of pathology when the release occurs[44].

A Novel *In Vitro* System to Characterize ASIC Function

Cell culture

Primary cultures of neuronal populations cells to construct and developmentally modify their own native ion channels, presuming normative growth conditions. Molecular receptors and ion channels sample the external environment in the same manner as the organism sensory modality of smell, by direct chemical assay that is concentration dependent on the source chemical's diffusion rate. Analogously, dilution of gaseous 'smell' is mirrored at the subnanometer size range within the

tiny volume of the neuronal surface where ions are taken-up; the cell is able to determine the strength of the overall 'signal' from an integrated sampling of the (ion) source-signal. The *in vitro* environment is ideal for the focused study of single ion channels; all of the external parameters are within the investigators ability to manipulate. The application of pharmacological agents in a dose and time dependent manner is the hallmark of electrophysiological studies.

Limitations of information content from culture

Objectively assessed, the *in vitro* environment does not provide the proper cellular context or chemical distribution system that is available *in vivo*. Simply stated, the native conditions can never be precisely replicated in a plastic dish. Some researchers call into question the validity of *in vitro* research regarding how realistic the conditions of development could be compared to *in vivo* conditions. Monitoring culture conditions carefully is currently a human investigator activity; there is no automation capable of assessing the health and nutritional needs of cells in culture.

The mouse OFB model system's anatomical origin

Figure 1: Cartoon of Brain and OFB regions

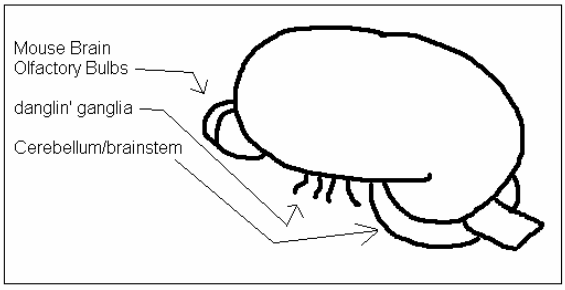

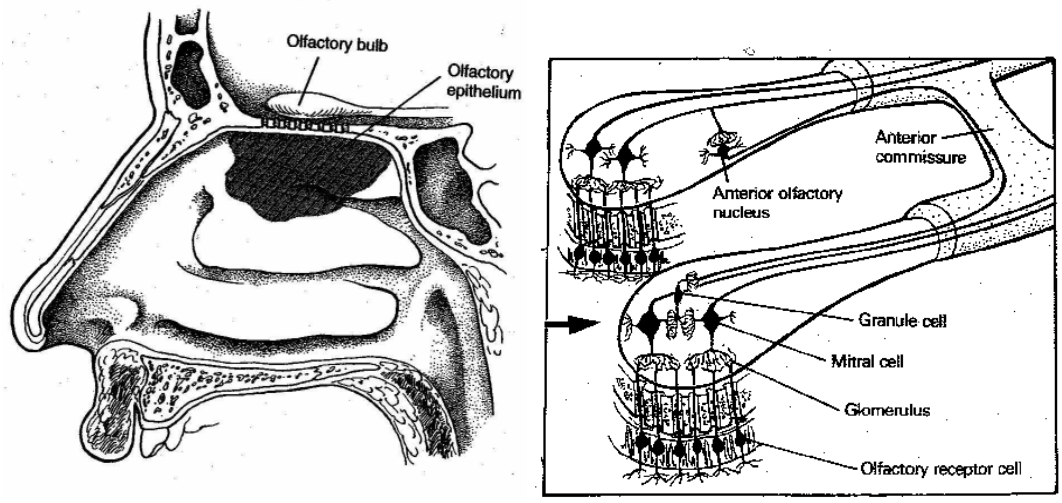

Cartoon of brain by author and OFB regions reproduced from Principles of Neural Science, 3rd Ed.: Fig.34-1, pg 513, Fig.34-3(inset),pg 514. The olfactory bulb (OFB) is distinct from the olfactory epithelium, (OE). As described below, several cell populations inhabit this brain region.

Cell types and anatomical regions of the brain and OFB

Glommerulus complexes connect to dendrites of mitral cells in the olfactory bulb region. Mitral cells, tuft cells, and juxtaglomerular cells also occupy the OFB region. The vomerulonasal organ (VNO) is most responsible for the function of olfaction processing. The main olfactory bulb (MOB) is the (olfaction) sensory routing center, taking the place of the thalamus in regards to culminating sensory inputs and sending meaningful responses to the organism's higher awareness. The accessory olfactory bulb (AOB) is virtually anatomically indistinguishable from the MOB. The rostral medial stream (RMS) are afferent sensory axons arriving from the nasal epithelium that are routed together along a common path. This anatomical feature is often studied as a retrograde pathway for neuronal injury.

The mixed morphology of these cell types (bipolar interneurons and multipolar receptors) combine to form a mosaic of sensory fields and inter-neuronal meshwork that modulate the sensory inputs from the incoming receptors from the nasal epithelium. The circular hollow anatomical structure of the OFB indicates that receptors present in this region may indeed be utilized for gustatory and

olfaction sensing, given the lumen-connection to the nasal sinus, lined with nasal epithelium (receptors).

Chapter 3: Materials & Methods

Primary Neuronal Culture

Primary cultures of mouse neuronal cortical neurons were prepared according to previous methods[17],[16],[45],[27]. The use of mice for the purposes of neuronal culture was reviewed and approved by the Institutional Animal Care and Use Committee of Legacy Clinical Research and Technology Center. Mice of the "Swiss-Webster" strain were obtained in a time-pregnant manner from the supplier, and were sacrificed on embryonic day 15 (E15) by halothane anesthesia followed by cervical dislocation. Brains of fetuses were rapidly removed and bathed in 4 degree C Extra Cellular Fluid (ECF) pH 7.4. Cortical hemispheres were separated from the midbrain and excess tissue was discarded. Meningeal layers (aka. arachnoid layer) of each cortical brain hemisphere were pealed away and discarded. Cortical hemispheres were then bathed in fresh ECF and inspected for residual excess tissue. Incubation at 37 degrees C for 10 minutes in 0.05% Trypsin EDTA dissolved in MEM media provided gentle enzymatic digestion of the extracellular scaffolding. After careful removal of enzyme, hemispheres were bathed in ~10 ml (excess) growth media to wash remaining enzyme away, then fire-polished glass pasteur pipettes were (mini-bulb) hand employed to triturate the hemispheres through three shrinking diameters, liquefying the tissue both gently and thoroughly. Cells were plated on poly-L-ornithine coated plastic 35mm dishes (Fisher) or onto round (coated) glass cover-slips (Fisher Scientific #12-545-86 25Cir 1D) 25mm in diameter. These glass slips fit the design of the calcium-imaging adaptor. Cell densities were 0.8×10^6 per dish and 0.5×10^6 per slip. Cells were maintained in an Incubator (Heraeus HERA Cell 150) at 37 degrees C at 5% Carbon Dioxide atmosphere with strong humidity provided by a sterile water pool. Cells were available for electrophysiology and calcium imaging after 12 days. Cells are plated in MEM, then 24 hrs later the media is carefully exchanged with Neurobasal medium with B27 supplement (10ml Gibco 50x #17504-044) and Glutamax (5ml Gibco 100x #35050-061). Cultures were fed three times per week.

MEM 500ml with 26mM NaHCO3 and 5.55mMGlucose; To MEM (1X) #11090, Life Technology; add 3.5gm/L: 1.75grams /500ml to make Glucose 25mM, then Add 5 ml L-glutamine (1:100=2mM final)(1%)[25], then Add 50 ml Horse Serum (heat inactivated, CELLect, ICN); (10%), then Add 25 ml Fetal Bovine Serum (5%); (Gibco #10082-139). pH was tested and adjusted by temperature-calibrated glass electrode, using calibrated pH standards. Osmolarity was adjusted by addition of sucrose to between 320-330 milliosmolar.

Electrophysiology

Single cell ion channel studies require electrophysiology to measure the electrical potentials that directly reflect the ion flux of the protein channel being studied. Application of a –60 mV tonic electrical "voltage clamp" produces an electrical circuit with ultra fine discrimination; any variation in the applied field is exactly the contribution of the ion channel's operational conductance; this is directly reflected in the "trace" of the electrical membrane potential; the channels may be observed opening and closing via the magnitude of the electrical current measured via computer instrumentation. The whole cell patch clamp method of electrophysiology is well established in this laboratory and identical equipment was utilized[46],[17],[16],[45],[27].

Procedures were also very similar; in brief; capillary tubes of thin walled borosilicate glass (1.5mm diameter; WPI, Sarasota, FL) underwent patch electrode (tiny syringe) construction via a two-stage puller (PP83 Narishige, Tokyo, Japan). Membrane potentials from whole cell patch clamp derived currents were obtained using an AxoPatch 1-D amplifier (Axon Instruments, Foster City,CA). Data filtration at 2 kHz, with data digitization at 5 Hz was done via Digidata 1320 DAC units (Axon Instruments). On-line acquisition performed by pCLAMP software (version 8, Axon Instruments). Once filled with intracellular solution, patch electrode had resistances between 3 and 5 MegaOhms and a diameter of 1-2 uM.

Whole cell recordings began five minutes after forming a strong (>5 Giga Ohm) resistance seal with an access resistance below 20 M Ohms. A multi-barreled perfusion system (SF-77B Warner Instrument Co.) delivered solutions in upstream proximity to the target cell in a very rapid (~2ms), computer-controlled manner.

Neuronal verification was performed via application of a potassium chloride solution (KCL); KCL 50mM, NaCL 95mM, pH 7.4, 320 mOsm. Voltage steps of –10 mV from the baseline holding potential were applied to verified neurons and samples with deviations of >10 % in the capacitances or access resistances were not included in data analysis. Data analysis occurred via exportation of the captured data-blocks into Microsoft Excel, then into SigmaPlot graphing software for further analysis. All data are expressed in mean with $\pm$ SEM; criteria for statistical significance via Student's T-test was set at $p < 0.05$. Dose response curves were fitted to the Hill equation to obtain $pH_{0.5}$ and IC_{50} values using the SigmaPlot software.

Standard ExtraCellular Fluid (ECF) solution (in mM): 140 NaCL, 5.4 KCL, 2.0 $CaCL_2$, 1.0 $MgCL_2$, 20 HEPES, 10 glucose, mOsm of 320-330, pH 7.4. Solutions of lower pH contained MES instead of HEPES, for better pH buffering. Voltage clamp recordings required pipette solutions (in mM): 140 CsF, 10 HEPES, 11 EGTA, 2 TEA, 1 $CaCL_2$, 2 $MgCL_2$, and 4 K_2ATP, mOsm 300, pH 7.3. Current clamp recordings required pipette solutions to use 140 KF instead of 140 CsF. Tetrodotoxin (TTX) at final 0.5 uM was added to all voltage clamp studies, and nearly all current-clamp studies; suppression of sodium current is the function of this treatment.

Specific pharmacological solutions: Amiloride (N-Amidino-3,5-diamino-6-chloropyrazinecarboxamide), refined venom of the tarantula *Psalmopoeus cambridgei* Psalmotoxin1 (PcTX or PcTx1) (Spider Pharm Inc. Yarnell, AZ), TPEN (N,N,N`,N` -tetrakis-(2-pyridylmethyl)-ethylenediamine). MCN is a

combination of calcium entry blockers that isolate the ASIC contribution from additional channel types; 5 µM nimodipine for L-type, voltage gated calcium channels, and 10 µM MK801 and 20 µM CNQX for blockade of glutamate receptors. Unless noted, all chemicals obtained from Sigma (St. Louis, MO).

Calcium Imaging

Fluorescent imaging dyes specific for the ion of interest (calcium) are incubated with the cells, and over time the cells absorb the dye. Later cells are imaged and treatments to perturb calcium entry are conducted. The colorimetric ratio imaging performed by the computer allows the calcium flux to be imaged and measured in "real-time". Some subcellular localization may also be interpreted via this technique, and will be critiqued in the results chapter. The instrumentation and methods of Fura-2 imaging are well known in this laboratory[46],[17],[16],[45],[27]. Cortical cultures on 25mm glass coverslips were washed three times in ECF pH 7.4, then loaded with Fura-2 fluorescent calcium imaging dye (5uM fura-2-acetoxymethyl ester) for ~40 minutes at room temperature. The sample was then washed three more times in ECF pH 7.4, then incubated in ECF pH 7.4 for 30 minutes before recording. These 25mm diameter coverslips were fitted into the perfusion chamber and mounted onto the inverted microscope (Nikon TE300 with Xenon lamp) with a 40X UV flour oil-immersion lens. A cooled CCD camera (Sensys KAF 1401, Photometrics, Tucson, AZ) obtained video images. Digitized images were acquired, stored, and analyzed using a Microsoft computer controlled by Axon Imaging Workbench software (AIW 2.1, Axon Instruments). The camera shutter and filter wheel (Lambda 10-2, Sutter Instrument, Novato CA) were also controlled via AIW for precise millisecond timing of shutter exposures of 340 or 380 nm excitation wavelengths. Emission of Fura-2 occurs at 510nm, and ratio 340/380 images were analyzed by pixel-averaging the ratio values within (user-chosen) defined borders of the video-feed image (the 'best' cells chosen in the field of view). Data analysis occurred via exportation of the captured data-blocks into Microsoft Excel, relevant data blocks were then exported into SigmaPlot

graphing software for further analysis. All data are expressed in Mean with $\pm$ SEM; criteria for statistical significance via Student's T-test was set at $p < 0.05$. Dose response curves were fitted to the Hill equation to obtain $pH_{0.5}$ and IC_{50} values using the SigmaPlot software.

Western Blotting

The property of antibody recognition allows the confirmation of ASIC proteins via the technique of western blotting; the separation of proteins from a mixed cellular lysate. Samples are loaded and run on an electrophoresis gel, and the gel-bands of interest are excised and then physically "blotted"; transferred onto a polyvinylidene difluoride membrane, which is then treated with antibody recognition reagents and visualized using computer isometric ratio imaging, determining gel-bands intensities (concentrations). Chinese hamster ovary (CHO) cells expressing ASIC1a and ASIC2a were used as positive controls, with beta-actin serving as a baseline. Adult (juvenile males) and embryonic samples (mixed genders) of the mouse olfactory bulb (OFB) were used, in addition to primary cultured (cortex) for comparison. Transfection of CHO cells via a Roche Kit was performed as described previously[47],[17]. Protein samples were obtained from ~50 ugram cellular lysates and the total protein concentration was determined using a Bio-Rad Protein Assay (Bio-Rad Laboratories, Hercules, CA) A polyacrylamide gel electrophoresis device (BioRad PowerPac Basic; 300 V, 400mA, 75 W) was employed using a denaturing 12% sodium dodecyl sulfate-polyacrylamide (SDS-PAGE) gel to resolve protein samples. Gels were blotted to vinyl membrane as described above. Membranes holding transferred (separated and somewhat purified) proteins were then probed overnight using primary (antibody) affinity purified rabbit polyclonal against ASIC (either 1a or 2a) protein (Chemicon International, Temecula, CA). Secondary labeling was done for 4 hrs via goat anti-rabbit horseradish peroxidase-conjugated antibody (Amersham Life Science, Piscataway, NJ) visualization of proteins was conducted using the NEN Western Blot Chemiluminescence Reagent (NEN Life Sciences Products, Boston, MA). Dilutions of primary antibody were 1:750, and for secondary 1:100. Positive

controls of wild type mouse, and negative controls included incubation with the absence of primary antibody[47],[17].

Immunohcytochemistry (ICC)

Cultured OFB cells and control cortical neurons populations were subjected to fixation, permeabilized, incubated with primary and secondary labels to localize ASIC proteins, then mounted using DAPI (4`-6-Diamidino-2-phenylindole) to visualize the nucleus. Samples (35mm dish) of cultured neurons were first washed three times in PBS, then fixed for 15 minutes using a 10% formalin (PBS) solution (2mls/dish). Three five-minute washings of PBS followed, then 5 minutes of quenching using a 2:1 Ethanol/Acetic acid solution. Three more PBS washes were followed by 20 minutes of permeabilization using 3% Triton-X detergent dissolved in PBS (2mls/dish). Three more five-minute PBS washes then preceded the twenty-minute incubation with a blocking buffer (in PBS) specific to the secondary host (150 uL/dish). Three twenty-minute PBS washes followed, then incubation with the primary antibody reagent (dil 1:750) (150 uL/dish) for 2 hours at room temperature (affinity purified rabbit polyclonal against ASIC (either 1a or 2a) protein (Chemicon International, Temecula, CA)). Three twenty-minute PBS washes followed. Incubation with the secondary reagent (dil 1:100) (150 uL/dish) occurred overnight at room temperature (goat anti-rabbit Fluorescein isothiocyanate (FITC). The next day three twenty minute PBS washes were done, then samples were mounted using a DAPI mounting reagent (VectaShield H-1200 Vector Laboratories inc. Burlingame, CA). Additionally, olfactory bulb (OFB) tissue slices of 400um thickness were obtained using a Leica VT 100 microtome and underwent similar procedures, for microscopic observation at several magnifications for anatomical and cellular localization.

Slides were mounted to an Leica DMLB inverted microscope supported by an MTI Optronics camera controller (DAGE, MTI, Michigan City, ID) and a Microcode II (Boeckeler Instruments, Tucson, AZ) digital image amplifier/enhancer. Fluorescence images were processed and analyzed using

BioQuant 98 Software (R&M Biometrics Inc.) Microscope objectives 10x, 20x were HC PL Fluotar type (dry), while the 40x objective was the PL Fluotar type (oil immersion). FITC (Fluorescein) Absorption 492nm/ Emission 520nm; Cy3 (Indocarboyanine) Absorption 550nm/ Emission 570nm.

Genetic Knockout animal verification

A professional animal care staff maintained the animal care facility. Animals were housed in either individual or family containment boxes of like gender. The boxes have inward and outward air pressurized airflow, with one full-volume air exchange every 45 seconds. The boxes are oversupplied with food pellets and water; there is no fasting or deprivation. Mating pairs and offspring were verified by tail snip donation for PCR analysis to verify genetic identity. Genetic knockouts of ASIC isoforms were used to verify by negative experimental result the findings of this project. Often males were used to preserve the females for further breeding. There are no known or detected gender differences in regards to ASICs. Genetic knockout strains of mice underwent identical procedures for electrophysiology, calcium imaging, and immunocytochemistry (ICC) as described above.

Chapter Four: Results

Morphology of olfactory neurons in cell culture

Neuronal cell culture is a powerful system for defining and characterizing molecular brain functions, including acid sensing channels. Olfactory bulb neurons are among the most readily available and potentially powerful cultured neuronal systems. However, prior to this dissertation, no tests had ever been conducted to determine the presence, activity, and isoform composition of ASICs in OFB cells. The goal of this work was therefore to investigate cultured OFB neurons as a potentially ideal model system to test the leading question regarding the heteromeric composition of functioning acid sensing channels in neurons.

I began by setting up a system involving the harvesting of olfactory bulb tissue from both neonatal and adult mice, dissociation of cells, and *in vitro* growth using normative primary culture conditions. As exemplified by Figure 2 (old 8), the cells obtained from the classically described OFB region prosper in culture. The visual refractility of the neurons was indicative of their health. Many interlacing branches of supporting cell were observed, indicative of neuronal morphology. Generally, such bright, multipolar and bipolar neurons were deemed the best candidates for ASIC currents. In figure 2 for example, eleven candidate neurons for testing were evident, including three near the lower left of the figure, the lone neuron at the top, and five centrally located. The two lower right cells were judged adequate for electrophysiological testing, but the cell on the far lower right was deemed a poor choice due to another cell partially obscuring it’s surface. Such were the typical considerations used in selecting cells for electrophysiology and characterization of ASICs.

Figure 2: OFB *in vitro* culture population

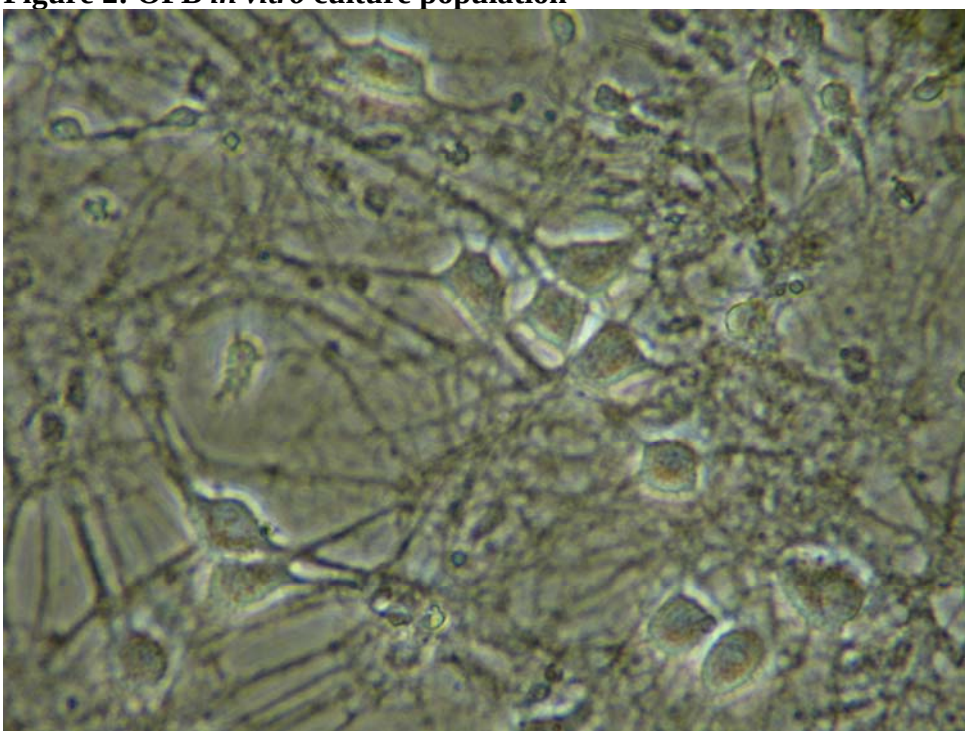

OFB *in vitro* culture population shown in Differential Interference Contrast (DIC) image at a 400x total magnification; brightfield microscopy. OFB cell populations grown on glasscoverlsips. Note the thick 'lawn' of supporting cells. The brightest outlined and most robust in girth are the neurons.

Verification of neuronal character: responsiveness to depolarization

Once the cells were morphologically assessed as neurons, they were then subjected to a voltage discrimination assay to quantify their neuronal activity under depolarizing conditions. A cell's neuronal character was routinely tested through an application of a drastically depolarizing saline solution that essentially forces any electrically excitable cell to undergo axonal discharge due to ion overflow. As shown in Figure 3 the negative and positive ions involved are measured under experimental conditions that assay the membrane potential and the subsequent current (ion) flow into the neuron. This procedure of neuron verification used a combination of voltage stepping and saline application (NaCl 99mM & KCl 50mM) to confirm neuronal activity. Excursions from the baseline (voltage-clamped at each 20 mV step) were due to membrane currents. Entry of negative

ions (anions) into the cell appeared as upward traces. Positive ion (cations) entry appeared as downward traces.

Figure 3: Neuronal verification

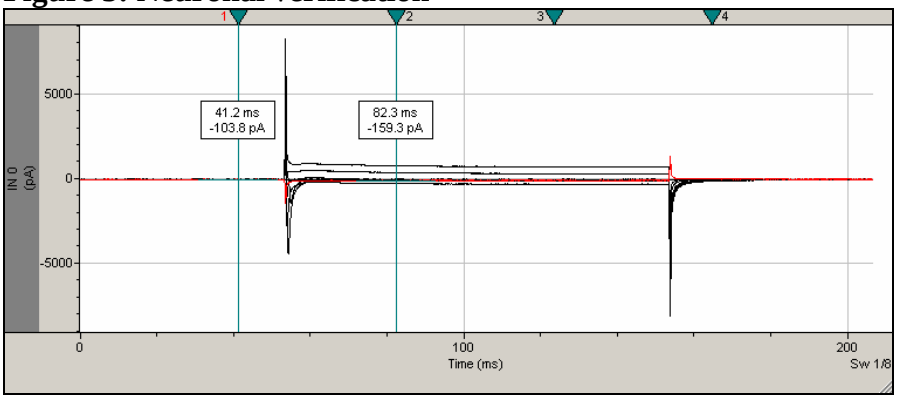

Neuronal verification plotted as channel current versus time in a single voltage clamped OFB cell. Downward traces (picoamps) shown here graphically exemplify the signature responses of all cation entry pathways, with ASICs being isolated by the pharmacological format of the assay. The majority of cells that appeared morphologically to be neurons passed this test of cell excitability.

Electrophysiological and pharmacological characterization of ASICs

To analyze acid sensitivity, Figure 4 shows such measurement of cation flow under voltage clamp (-60 mV) conditions with TTX present to block sodium channels and the aforementioned MCN cocktail whose purpose is to block all other non-ASIC calcium gating channels (see Methods for further description of these agents). Such results as shown in Figure 4 were the first to detect functional pH dose responses ASICs in mouse OFB neurons.

Figure 4: Single OFB Neuron pH activation

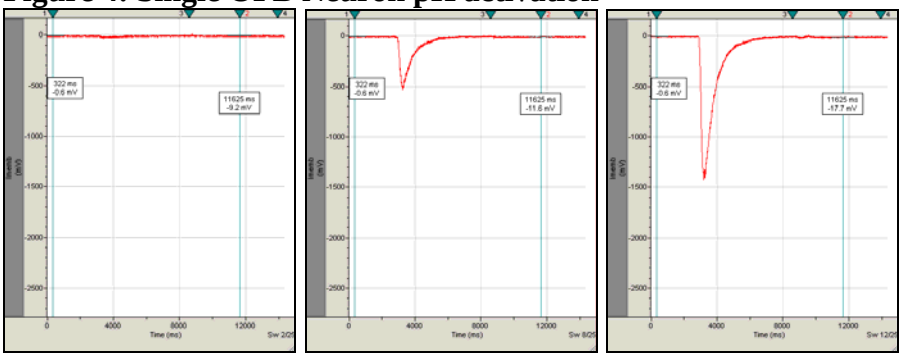

pH 7.4 pH 6.5 pH 5.0

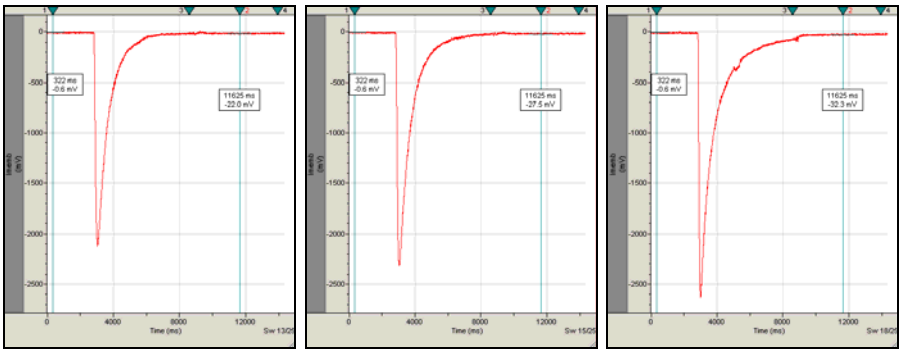

pH 4.5 pH 4.0 pH 3.5 (max)

Single OFB Neuron pH activation illustrated by graphing membrane current versus time with increasing acidity (pH from 7.4 to 3.5).

The sequence of six images illustrated in Figure 4 (six photo figure) qualitatively shows increasing ASIC responses with each pH step. To further quantify this behavior, Figure 5 shows the response of a second OFB neuron to a similar series of pH steps. In this case, the traces of membrane currents have been superimposed to make obvious their relative amplitudes. The trace of greatest amplitude (at pH 3.5) is highlighted in red color. When the amplitudes in such experiments were plotted versus pH (Figure 5, right-hand graph), the amplitudes generally showed the robust pH dependence expected of acid-sensitive channels, but of course, being data from but a single neuron, it was not clear that this biophysical behavior was representative of most OFB neurons. Therefore, to expand this study of pH sensitivity, an extensive series of pH dose-response experiments was conducted.

In the series of experiments that followed, single cells were subjected to lengthy recording sessions (~40 minutes) of step-wise pH applications (Figure 6). Both steps of increasing and decreasing pH were used, with appropriate washes.

To increase the number of recorded measurements, both the number of cells was increased as well as the number of pH steps, culminating in the construction of Figure 6, whose downward pointing traces shown directly correspond to the inward cation flow as represented by (pA) membrane current amplitude increases.

Anatomical and morphological views of neuronal population

Figure 5: Single OFB neuron pH dose response

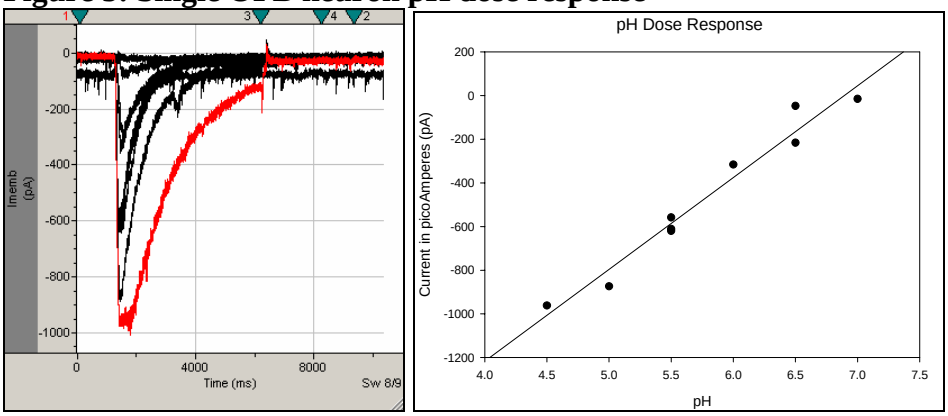

Single OFB neuron pH dose response graphed as Membrane current versus time. Left: Traces of ASIC activity upon pH application from 7.4 to 4.5 (red) Right: Dose response plotted as a linear relationship to pH decreases

In such a single OFB neuron dose response linear relationship, note that as the pH decreases (more protons), more current (shown on the Y axis as more negative) enters the cell. The figure shown here illustrates the baseline current straight along the top, and with each sweep the pH decreases (more proton concentration), and thus stronger currents are exhibited. Exemplified by the trace (in red) shown at the right, the maximal response of pH 4.5, correlating the maximal current in the right hand graph. The traces and graph originate from the same data file.

Recovery from signal saturation

Note the recovery spike when the channel is fully closed in the right hand lowest (red colored) trace, the slight upward positive flow is often exhibited in these circumstances of channel desensitization upon saturation of maximal signal. Also shown on the above linear dose response representation is the near-zero current that matches with the most normative physiological (pH 7.4) condition.

Figure 6: Single OFB pH dose of long duration

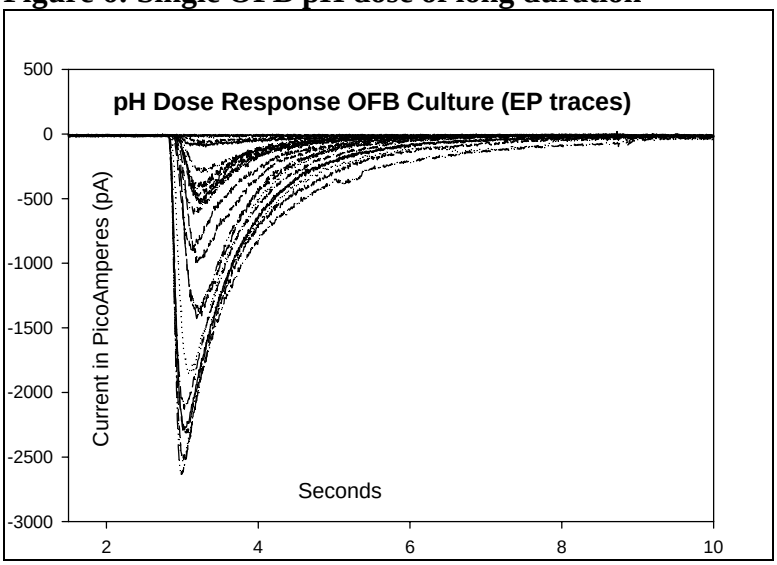

Single OFB pH dose of long duration plotted as membrane current (pA) versus time, with pH application at the standard one second marker. All traces are sown overlaid for ease of visual comparison of the pH current responses.

Confirmed OFN Neurons via the KCL test (50mM) was followed by relaxation duration, then treatments of pH were applied and current amplitude measured. Relaxation times of 90seconds to 2 minutes per each sweep/trace were performed. Next of interest was the current relaxation time. OFB cells confirmed as neurons via the KCL test (Figure 3) were tested for relaxation duration. Treatments of pH were then applied and current amplitude measured. Relaxation times of 90seconds to 2 minutes per sweep/trace are shown here. The lengthy relaxation directly supports the identification of the channel as the ASIC 2a isoform.

ASIC pH dose response relationship

The pH dose response relationship study was next conducted, in parallel with pharmacological manipulations designed to illustrate the ASIC isoform composition. A series of OFB populations were harvested, grown, and assayed using the techniques described above.

Figure 7: pH Dose Response Profile

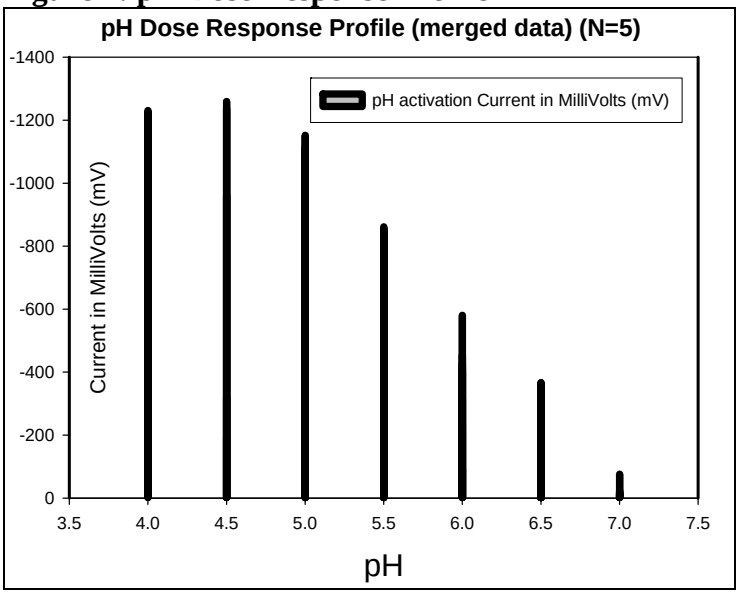

pH Dose Response Profile displays here in bar graph format the membrane current in millivolts, the so-called 'raw' cation flow, shown here as a linear relationship, with a plateau in the pH 5-4 range. The response more than doubles from pH 6.5 to pH 5.5; and this response is a hallmark ASIC molecular attribute.

The current saturation shown here in millivolts is differently illustrated in figure 8, which depicts in bar graph format the membrane current in picoamps, which is relative to the rate of ion entry. (Further studies below will address the related issue of the gating of both sodium and calcium ions by this population of ASIC channels.)

Figure 8: pH Dose Response Bar Summary

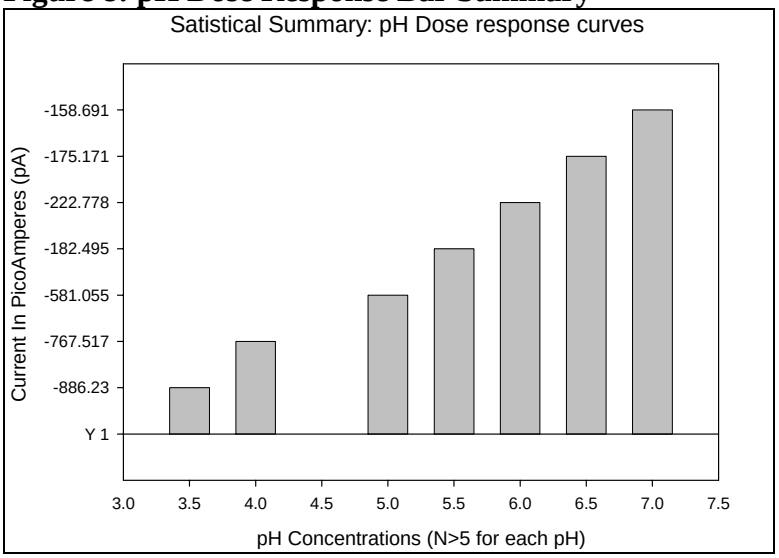

pH Dose Response Bar Summary here represents a stepwise application of greater proton concentrations, shown in figure 8 from right to left, correspond with increasing (negative) current amplitude as pH decreases.

The current in picoamps is the instrumentation's measurement of the discrimination from the (applied) 'clamped' voltage of -60 mV. The column for pH 4.5 had only three data sets, so was not included. More than five extended sets of recordings were used to construct Figure 8, which strongly indicates a linear positive slope of unity when plotted picoamps versus decreasing hydrogen ion concentration (pH). Figure 8 illustrates several (ion channel) properties that are specific to the sodium/calcium gating subfamilies and ASICs; the known role of the ASIC1a isoform as the amplitude determiner was correlated to other ASIC studies, and these results here support the conclusion of ASIC1a being present and indeed gating the so-called 'raw' current shown above. These representations of the OFB neuronal membrane current picoamperes (Figure 7) indicates the rate of cation flow, while the membrane current in millivolts (Figure 8) indicates the actual amount of cations that cross into the neuron.

Shown in figure 8 in bar-graphical format, the rate of cation entry is linear. This validly suggests that the (ASIC) isoform composition of remains constant for the ASIC1a isoform. If the number of ASIC 1a isoforms were to increase in the

channel as a consequence of increasing (the neuronal microenvironmental) pH, then the slope of the cation flow rate versus pH would not be unity. Note that in figure 8, the Y axis depicts more current as the scale proceeds downward. This format is intended to highlight the standard linear slope relationship.

Given this body of evidence, qualitative curvature of the traces across the series of replicates confirmed the pH sensitivity of OFB neurons. The main functional role of ASICs, that of pH sensitivity, was thus confirmed. OFB neurons thus prove to be a robust cell culture system to study the electrophysiology of a neuronal ASIC.

ASIC pH dose response: sigmoidal curve fit to Hill Equation

With this model ASIC now in hand, an important biochemical principle comes into consideration to better resolve the relationships between the neuronal ion channel composition and it's physiological activity. This principle, the Hill relationship, is typically graphed in a logarithmic to logarithmic relationship to clearly illustrate the slope, to help reveal the number of subunits involved in the cation movement. Shown in figure 9, the Hill equation was curve-fit as a function of relative amplitude plotted versus pH. The sigmoidal shape of the plotted data was generated from a large number of data sets.

Figure 9: ASIC sigmoidal curve fit to Hill Equation

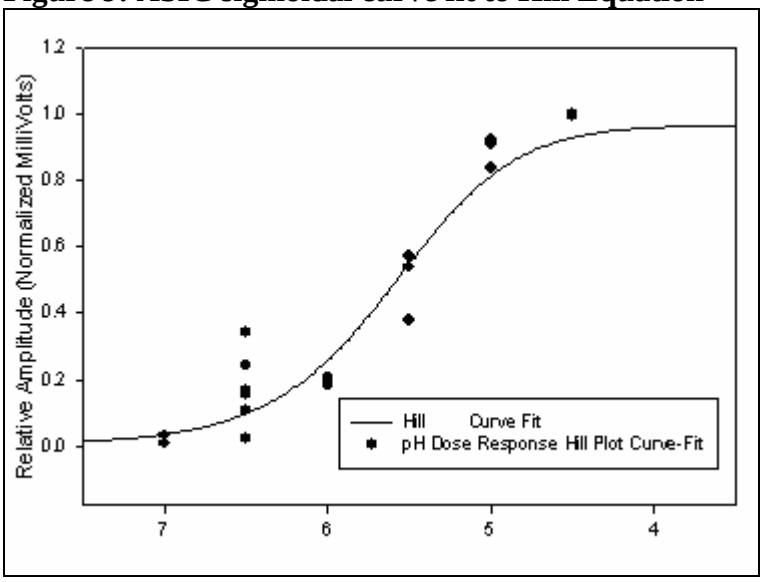

ASIC sigmoidal curve fit to Hill equation represents subunit cooperativity even without using specialized kinetic studies; these data sets are amassed here to present the full range of ASIC activity, presented in normalized millivolts plotted versus pH applications.

The curve was especially informative at its the upper and lower boundaries since these reflect responses of the differing subpopulations of ASIC isoforms. The position in the curve at which half the channels were active, at the midpoint along the Y axis-response, had a value of 5.5 pH. Interestingly, that is equal to the published and widely accepted value for the ASIC 1a + 2a isoform composition value (see figure 10).

Further dissection of the date by of normalization of the channel's current in millivolts (Figure 9) establishes a standard function; division of each activity amount by the maximal, which equates to a percentage of overall activity for the entire (data-set) neuronal population. The lower boundary of this relationship shown here (left lower curvature) depicts channels normal physiological pH values of 7.4 to 7, moving into the ASIC activation along the X axis with more acidic pH values.

The relative amplitude shown on the Y axis in Figure 9 reveals virtually zero activation of the channel corresponding to nominal physiological pH, further supporting the established functional role of ASICs in sensing the neuronal microenvironment pH and enacting signal transduction to relay that information pertinent to survival to the cell.

The upper boundary of this relationship shown here (right upper curvature) illustrates the pH range from 5, becoming even more acidic as the curve moves to the right along the X axis. The corresponding relative amplitude graphed in normalized millivolts versus the X axis increasing acidity; decreasing numerical values of pH; has value

The largest number of measurements were taken at pH 6.5 column, since that pH was generally crossed twice in the traversal of pH measurements. Tellingly, the cluster of the data points at 6.5 pH on the Hill equation curvature showed a wide distribution, from essentially zero to forty percent activation (0.4 relative amplitude). This likely reflects the widely varied output that is a functional consequence of a heterogeneous population ASIC's, each subclass of which has a distinct response near physiological pH. Thus, by this interpretation, OFB neurons display an interesting variation in the heterogeneity of ASIC populations that shapes the repertoire of current responses to pH fluctuations in the vicinity of physiological pH.

Half-activation is a significant secondary biophysical channel property

The half-activation values (pH_{50}) listed in figure 10, are important in terms of physiological functionality. These values directly reflect the pH sensing gradients that these ASIC isoforms are specific for; the overlap of sensing functions (redundancy) in both expression and detection/ activation thresholds, and in this case, half-maximal activation values, strongly supports the hypothesis of overlapping combinatorial (isoform based) micro-environmental sensing being

conducted by these cell types, primary cultured olfactory bulb neurons of the mouse animal model.

Figure 10: ASIC isoform half-activation pH $_{50}$ values

ASIC1a	5.8
ASIC2a	4.5
ASIC(1a+2a)	5.5

Amiloride blockade confirms sodium channel character

The general sodium channel blocker amiloride was employed in a dose response manner and a summary graph is depicted in figure 12, and a total blockade of the channel shown in figure 11 as an electrophysiological trace display. As the pH sensitivity is tested with an applied dose of pH 6.0 in this figure, the measured current in picoamps increases to –400 pA, directly indicating ion movement as represented by the vertical downward (more negative) outline of the trace; the signature ASIC current trace displayed here. The horizontal line indicates a complete ion blockade, with negligible current during the concurrent application of ASIC activation pH combined with amiloride. Subtle ion movement of both measured responses (drug treatments and washes) is evident at the start and stop time points of the flow application; the so-called ‘bump’ of the channel closure is seen in both traces shown in figure 11.

Figure 11: Amiloride Blockade of OFB neuron

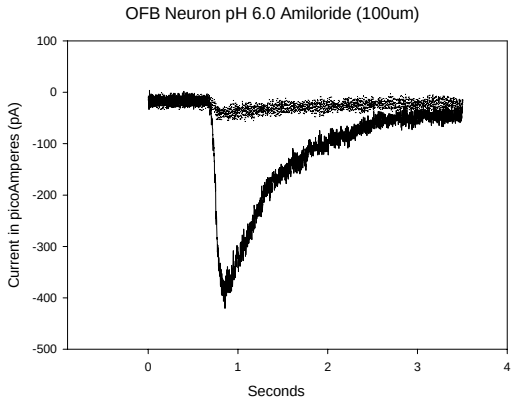

Amiloride Blockade of OFB neuron shown here illustrates the lower trace as pH 6.0 activation of approximately 400 picoamps. The top (flat) trace shows complete blockade by amiloride (100 micromolar). Note: Other traces not shown for clarity.

Sufficient evidence of this agent's activity in regards to the ASIC systems was documented to verify the channel in question as a sodium channel family member by definition of their pharmacological responses. The half-maximal blockade concentration required, as shown in figure 12, is 1 micromolar. The activity of this agent in the ASIC system is well understood. A single amiloride blockade is shown in figure 11 for clarity; as a dose response series would appear very similar to figure 6, with multiple traces overlaid on a single graphical display. A dose response series for amiloride using nine concentrations is graphically depicted in figure 12.

Figure 12: Amiloride Dose Response Curve (N=9)

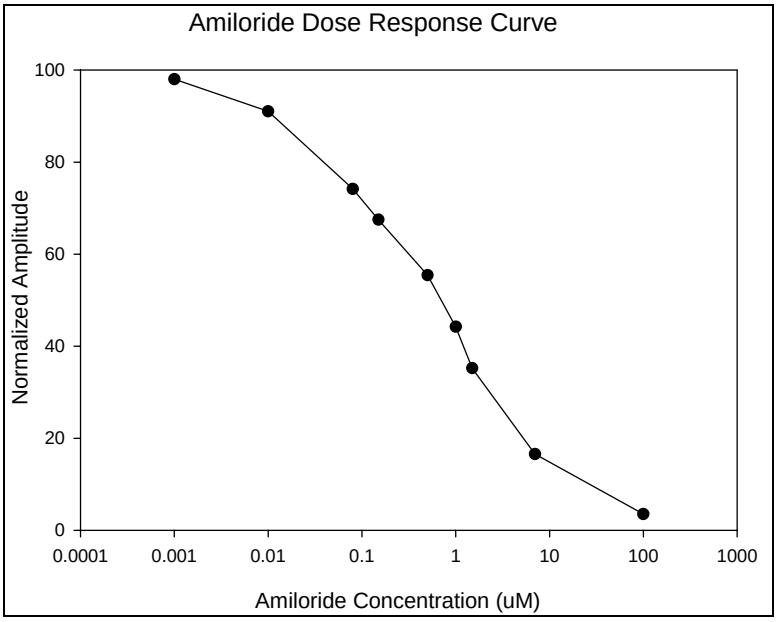

Amiloride Dose Response Curve (N=9): normalized amplitude versus amiloride concentration verified known efficacy of this drug treatment.

The general sodium channel amiloride was an effective ASIC blocker. The series of nine amiloride concentrations shown here graphically display the linearity of the pharmacological application relationship of amiloride, supporting its continuing use in electrophysiological studies in regards to it's reliable activity. Being a general sodium channel blocker, the measured pharmacological responses to this

chemical agent further corroborated the presence of functioning ASIC in cultured mouse OFB neurons.

The specificity of PcTX confirms ASIC activity

The pharmacological response of OFB neurons to application of the drug PcTX, was found to be qualitatively identical (seen as a flat line) to the amiloride response in figure 11 and 12. Further trials of the effects of PcTX yielded the dose response relationship plotted in figure 13. The extreme sensitivity of the ASIC system to this particular agent is evident in the dosage sensitivity of PcTX being in the nanomolar range, a well-accepted characteristic of ASIC1a.

Figure 13: PcTX Dose Response Curve (N=6)

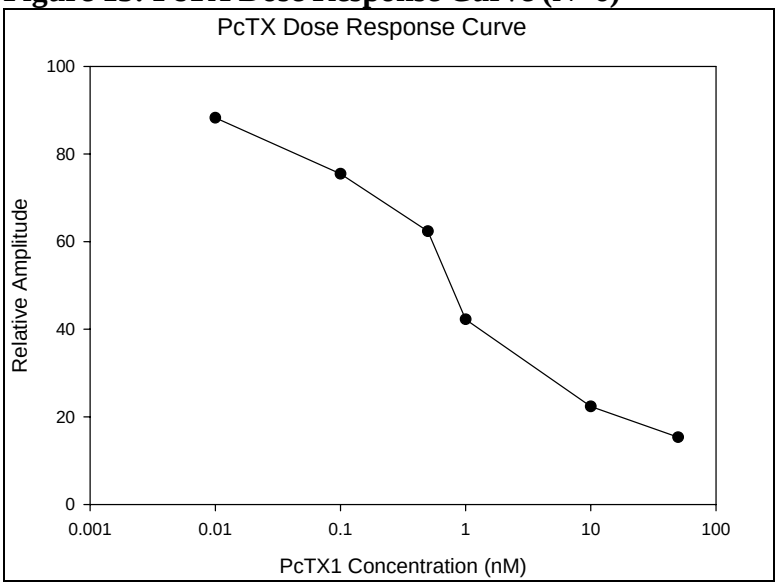

PcTX Dose Response Curve (N=6) reveals nanomolar blockade effectiveness versus ASIC1a containing channels.

The specific ASIC channel blocker PcTX displays an effective ASIC blockade, with a half maximal blockade at 1 nanomolar and total blockade at 100 nanomolar concentration. The extreme potency of this chemical demonstrates the effective usage as a possible therapeutic agent, targeting ASIC related pathologies.

Zinc potentiation confirms ASIC 2

Previous studies in this laboratory have shown the potentiation effect of zinc in regards to ASIC isoform composition, specifically the inhibition of ASIC 1a isoforms and the increase in current when ASIC 2a isoforms are present. The half-maximal activation value of zinc is between 100 and 110 micromolar, and specifically targets ASIC2a containing channels. The inhibitory effect that zinc has on the ASIC1a isoform component of the channel population examined has been verified with these mouse OFB samples. As shown in figure 14, the increase in amplitude shown in the light grey colored trace represents 300 micromolar concentration zinc, which is three times the half maximal value of 100-110 micromolar, indicting certainty of activation though application of this concentration value. Fluid flow application of pH 7.4 washes were always conducted to preserve fidelity of experimental results.

Figure 14: OFB Neuron Zinc Potentiation

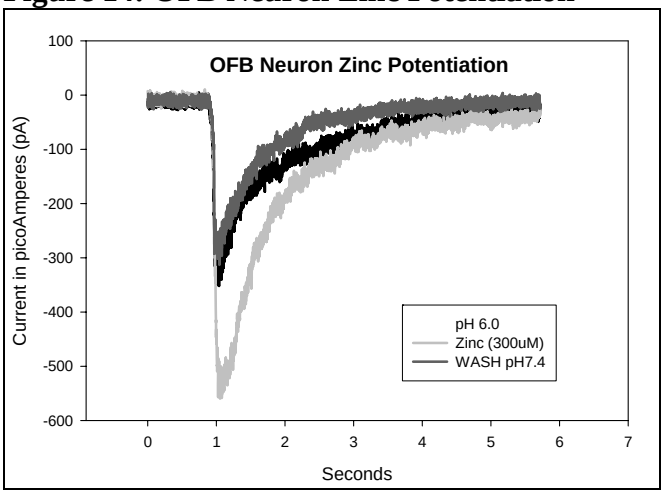

OFB Neuron Zinc Potentiation: Sweep 1: middle (black): pH 6.0. Sweep 2: lower (light grey): Zinc (300uM). Sweep 3: (grey): washes. Note: only three traces shown for clarity.

These trials indicated the participation of ASIC heteromeric channels.

Zinc treatments consistently increased ASIC current amplitude, a pharmacological process called potentiation. Such zinc potentiation confirmed the presence of ASIC2a isoform dominant channels. This result alone would indicate ASIC2a

homomeric composition, although when taken together with the previous findings of this dissertation, the heteromeric channel composition of the OFB neuronal population is verified.

Zinc chelator TPEN also potentiates ASICs

TPEN alone will potentiate ASIC 1a, 1a and 2a heteromeric combinations, but not channels that contain ASIC 2a + ASIC 3 or ASIC 1b splice isoforms. The results presented here indicate the activity of heteromeric ASIC 1a +ASIC 2a containing channels. When combined with the above zinc findings, the valid inference to be concluded is that of ASIC1a +ASIC 2a heteromeric channel are the major population composition in the mouse OFB.

Figure 15: OFB Neuron TPEN Potentiation

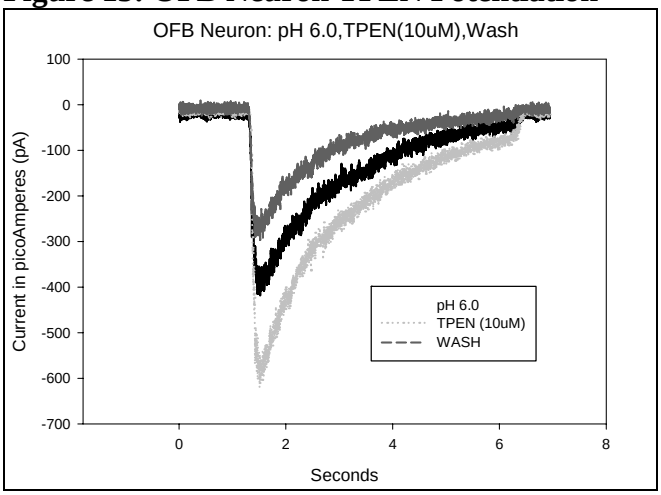

OFB Neuron TPEN Potentiation: Sweep1: middle (black): pH6.0. Sweep 2: lower (light grey): TPEN (10uM). Sweep 3: (grey): washes. Note: only three traces shown for clarity. Many pharmacological manipulations were performed, with appropriate washings between treatments.

The observational origin of desensitization

The clinically described neural activity of “spreading depression” refers to lowered neural activity (less action potentials) and was first established as a neurological marker several decades ago. The classic phenomenon of “spreading depression”, first described by Artistide Leao in 1944, describes what was long thought to be artifact of the technology at the time; a moving wave of neuronal *in*-activity, the

absence of action potentials moving from one brain region to another, correlating with the zones of injury. Traditional neuropathology therapeutic strategies are centered upon what produces clinical results, with the underlying inactivation mechanisms largely being unknown. It was therefore of interest to examine ASIC 2a functional rate of recovery from the desensitizing effect of full signal saturation.

Desensitization parameters illustrate ASIC isoform composition

Channel property kinetics requires a brief duration when the channel must remain closed. This desensitized state entails that ligands normally activating the channel would be ignored at the molecular level, as conformational changes may be masking the binding site until the channel recovers. The established recovery duration after ASIC acidic exposure activation is 2 minutes, to allow for maximal responses in the next round of activation. The rapid mechanism of ASIC1a recovery differs from ASIC2a, which has a much slower recovery time.

The so-called refractory period following channel activation cannot be avoided. Individual channels must perform this action. However, the entire population of channels may not respond in an identical manner; that is, all channels do not recovery at the same rate. Note that the sub-population of ASIC channels that recovery more quickly need not be in the larger population of channels that were activated by the initial acidic exposure.

The procedure used to measure recovery from desensitization experiments was to apply a channel activator, then at shorter and shorter intervals (less than 2 minutes) assay the current with another acidic activation attempt (Figure 16). Typically, a certain percentage of channels would be expected to be available for activation, even down to very short time intervals after initial activation. Some of these channels were perhaps not activated in the initial exposure, as expected if all channels are not constructed with equal kinetic properties.

Figure 16: ASIC Desensitization profile

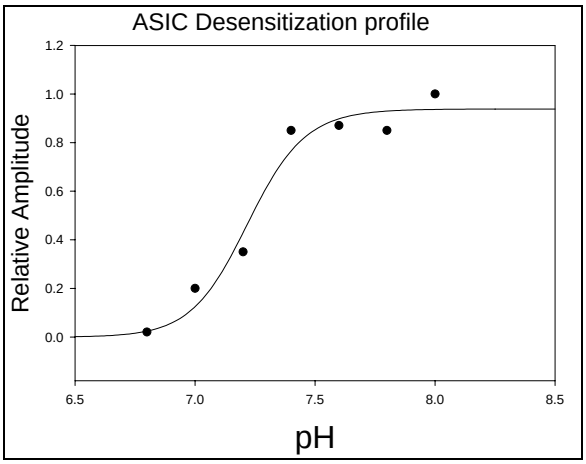

ASIC Desensitization profile shows maximum signal saturation of ASIC protein; the desensitization plateau is established after surpassing a physiological pH of 7.4, went into the pH 8 range. The relevant mammalian physiology pH ranges are displayed here.

Voltage dependence and the reversal potential elucidate the ion

Fundamental biophysical principles are employed in the methodology of electrophysiology. Utilizing a stepping voltage clamp application, the holding potential of the cell is held constant by the applied field and the current in picoamps is measured. This was repeated for seven voltages at 20 millivolt increments. Figure 17 graphically depicts the linear line fit function for this procedure as crossing the X axis at negative forty millivolts (-40mV). The centrally joined axes of this graph (Figure 17) enable the relationship to be readily visualized and corroborated by standardization. The reversal potential is the X axis intersection of the linear fit function; the amplitude of which numerically demarcates the gating of calcium ions as described previously [3]. The reversal potential is distinct for each (in this case divalent cation) ion type; both the sodium and calcium were confirmed as gating ions in mouse neuronal ASICs during the course of this dissertation. Thus, the gating of calcium confirmed the presence of the ASIC1a isoform, further illustrating the heteromeric isoform composition of the mouse OFB neuronal population.

Figure 17: IV Curve of OFB Neuron

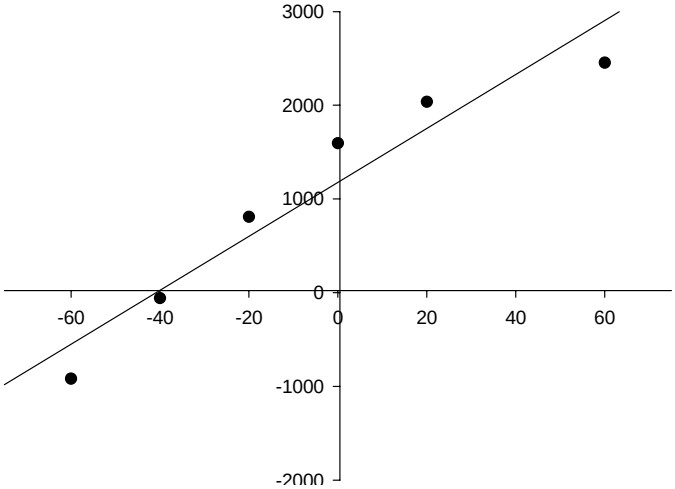

IV Curve of OFB Neuron: Current (I) in picoAmps (pA) divided by the holding voltage in milliVolts (mV). Traces with pH 5.0 application and stepwise 20 mV increments. The centrally located origin of axes allows the plot to reveal the reversal potential, which is biophysically indicative of the ion type. This IV curve confirms the gating of calcium in mouse OFB neurons, using methods described previously [3].

Activation of ASICs to examine heteromeric composition

The maximal activation of ASICs conducted at pH 4.0 was studied in further detail in figures 18 and 19. This examination of the maximal activation reveals some details about the biophysical saturation of the signal, in regards to the 'relaxation' of the curvature, the leftward closing of the channels population shown in figure xx below. The curvature qualitatively reveals that between 1500 milliseconds and 2000 milliseconds, the majority of the ion channels reduce their maximal picoamp current output below the –1000 mark, moving upward towards zero. Another interesting feature of figure 18 is the lack of full recovery by the neuron; the current does not return to the full basal level that was measured prior to pH application, as clearly delimited by the horizontal trace.

Figure 18: ASIC Max Activation at pH 4.0

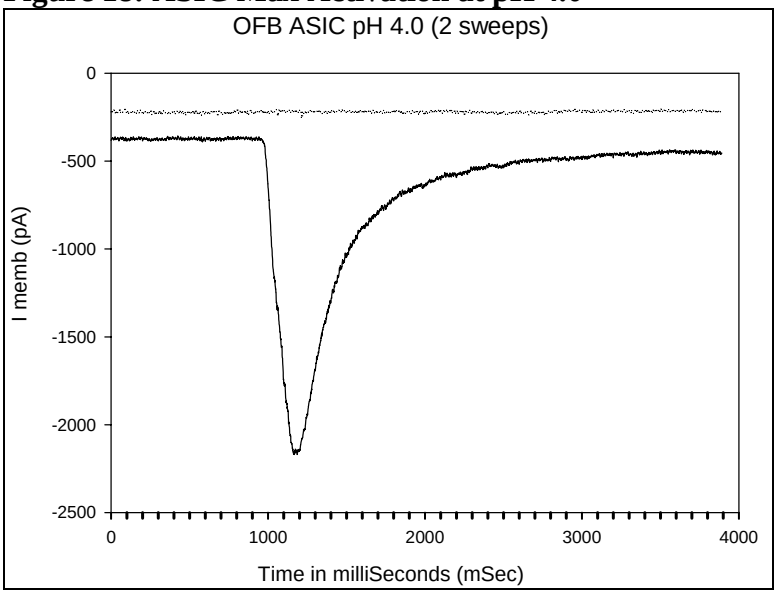

ASIC Max Activation at pH 4.0: OFB Neuron showing pH 7.4 (flat trace) and maximal activation at pH 4.0. Long duration of saturation required (right upward slope of trace) is indicative of heteromeric channel composition.

From preliminary investigations (data not shown), it was determined that ASIC populations did not respond to pH changes in the expected mammalian physiological range 7.2 to 5.5 as the homomeric ASIC 1a model of activation describes. A refined strategy was therefore used by which electrophysiological recordings, doses, and treatments, with pH 3.5 being set as the lower experimental boundary. Setting the pH near this lower boundary ensured that the majority of the channels were heteromeric in OFB samples. While being unable to technically confirm or refute the precise number of subunit (isoform) participants in native mouse neurons, these data sets, when correlated, strongly suggest heteromeric channel character.

Further examination of the very apex of the pH 4.0 activation trace (Figure 18) revealed the nuances of the ion channel's function in regard to the saturation of signal and the very instant in time that the channel ceases cation influx activity and begins a decline in channel openings. The latter can be seen to occur in figure 19 during the 1.16 to 1.20 millisecond timeframe on the X axis. The jagged profile of the measured picoamp current directly correlated to small subpopulations of

channels opening and closing at slightly different rates.. The magnification of this trace also showed how short-interval sections of plateaus during time ranges 1.05-1.06 and 1.10-1.11 were revealing this closing behavior of ion channels. A homogeneous population would not generate the short plateau sections seen here.

Figure 19: ASIC Imemb (pA) Saturation (2mSec) closeup

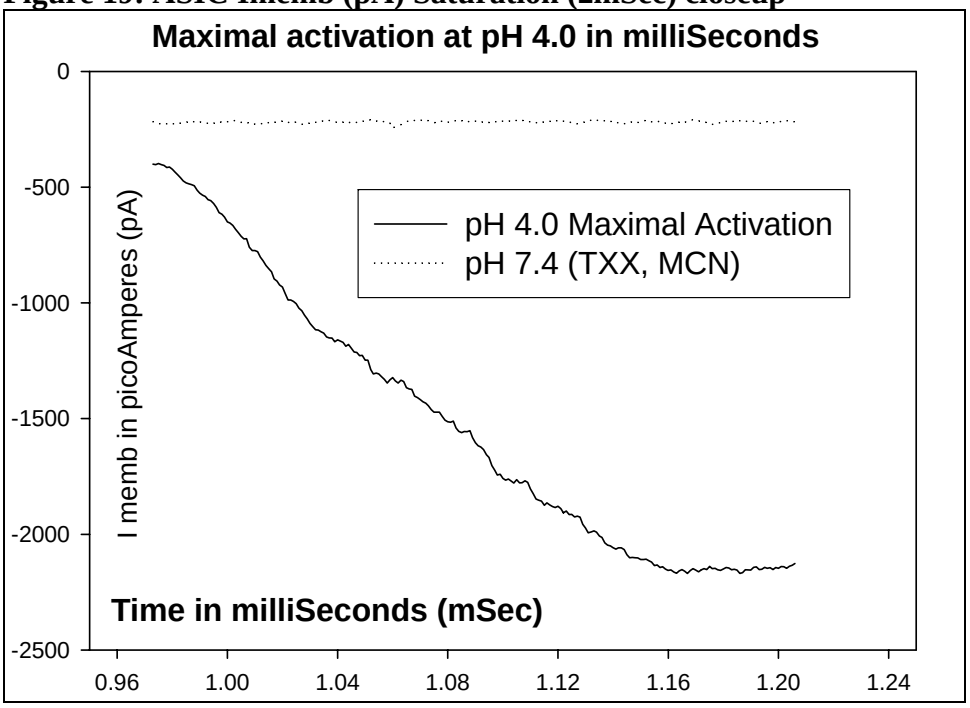

ASIC I memb (pA) Saturation (2mSec) closeup: An extreme temporal resolution shows the saturation of calcium gating performed by ASICs (OFB neurons) during just 2 milliseconds (0.96 until 1.16). This graphic corresponds to the very apex of the virtually vertical trace seen above in figure 18.

The inferences drawn from this 45 degree slope is that maximal usage of available ASICs for calcium gating is occurring up to 1 .04 milliseconds. After that, subpopulations of channels begin closing and soon, at 1.16 milliseconds, a complete plateau of maximum activity is sustained for approximately 0.04 milliseconds.

Visualization of calcium entry demonstrates ASIC1a activity

Calcium imaging illuminated ion flux in living cells, confirming the presence of ASIC 1a isoform through its known function of calcium gating under acidic pH

application, figure 20 reiterates the procedure for neuronal verification under the auspices of calcium imaging.

The prominent functional role of calcium in neuronal physiology is an enormous field; specifically for this dissertation, the of calcium gating conducted by the ASIC 1a isoform holds functional relevance in several neuronal pathologies, making the study of ASIC heteromeric combinations a vital step toward elucidating the full range of modulation functions performed by ASICs. This dissertation investigated the presence and activity of ASIC isoform heteromeric cominations of the ASIC 1a plus 2a isoforms; the subtle yet revealing biophysical differences incurred through the inclusion of the ASIC 2a subunit and its established ability to alter the so-called secondary biophysical parameters such as recovery from densensitization and refractory period duration. These issues are examined in this work, and a sizeable body of validly strong experimental results were obtained during the preparation of this dissertation. However, only a small portion of representative results are presented herein in figures 20 through 26 that support the ASIC 1a + 2a heteromeric combination as being the dominant protein subunit quanternary amino acid structure, also known as multermericity.

Figure 20: OFB neuron verified by KCL

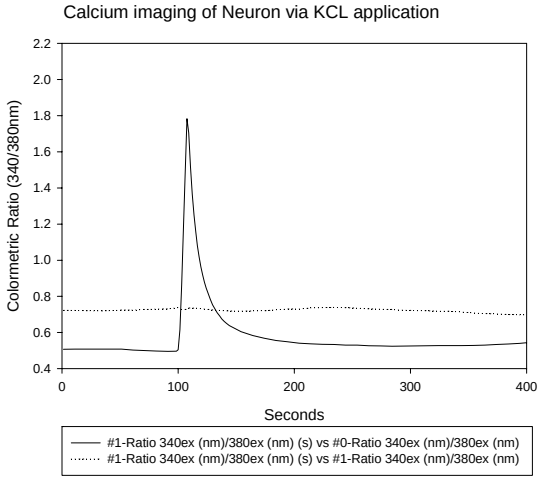

OFB neuron verified by KCL: Colormetric ratio versus time shows here the calcium influx spike triggered by KCL application superimposed with a pH 7.4 application shown as horizontal line.

The calcium imaging result shown in figure 20 is a graphical overlay of the response of a confirmed (50mM KCL) OFB neuron (solid line) compared to the dotted line that indicates no treatment with activating solution. Note the level of activation (calcium flux) from 0.7 to a maximal spike of 1.8, indicating that a sufficient change (increase) in the excitation to emission ratio. This amount of relative increase, of about 1 is a strong signal, given the activation by KCl. This procedure was a standard consideration in choosing OFB neurons for further assays that would reveal further insights to their isoform compositional character. Confirmation of ASIC1a activity through calcium gating triggered by acidic pH application was obtained through direct visualization of living OFB (*in vitro* cultured) neurons

Figure 21: OFB Neuron fluxes Calcium with internal control

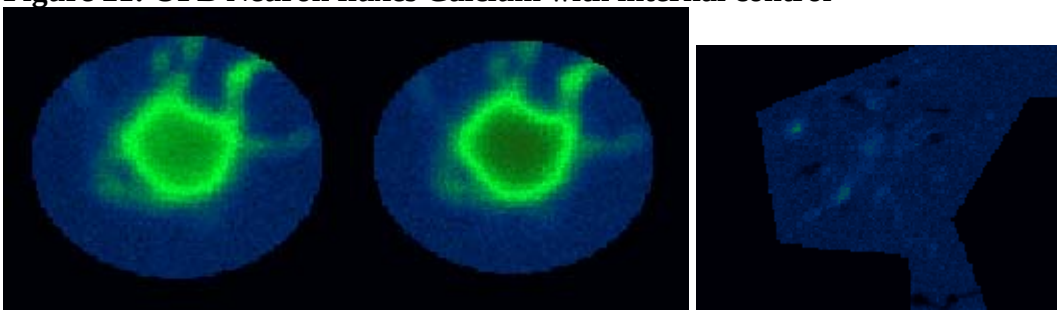

Time A Time A+300 millisecs non-responsive cell

Neuron fluxes Calcium with internal control: Membrane localization is illustrated in these "freezeframe" images from the same glass coverslip that were single-frame captured from digital movie recordings of microscopically imaged cells.

PCTX blockade is effective in conjunction with this calcium imaging assay, characterizing the activity precisely to the ASIC 1a isoform.

Figure 22: Calcium entry in OFB cultured cells

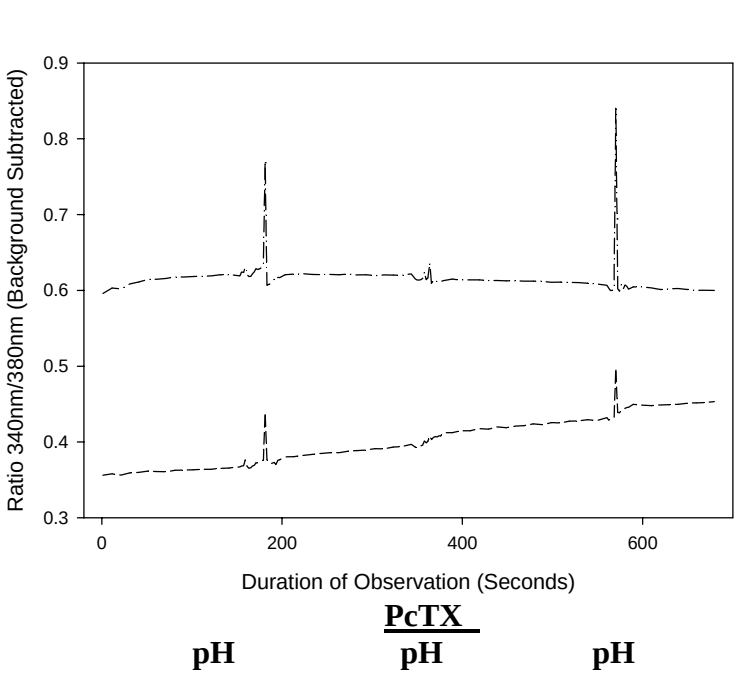

Calcium entry in OFB cultured cells shown through colorimeteric ratio imaging using Fura-2 dye in healthy cultured OFB neurons. The ASIC 1a specific antagonist (blocker) PcTX application is depicted as a bold line in the center of the recording, while the pH activations are shown as grey highlighted zones corresponding to their application during the recording duration. Note extended ten full minute duration of this assay.

Two OFB neurons are show in figure 22, with similar responses that differ in magnitude. The observed increases of 0.1 to 0.3 in the colorimetric ratio is within the realistic physiological range of these pharmacologically isolated ASIC proteins, and these results of this issue comparable to literature [5,6]. In these experiments, precisely delivered, software controlled perfusion barrel application of pH treatments occurred at 180, 380, and 580 seconds. The top calcium trace (dotted/dashed) shows a slight 'bump' at the 380 second time marker, which corresponded to application of 50 nM PcTX dissolved in ECF pH 6.0. The bottom trace (dashed) shows complete abolishment of any current during the PcTX application, confirming in that cell at least, the presence of homomeric ASIC 1a channel population. Suppression of calcium entry by PcTX blockade of the ASIC1a isoform effectively ceased calcium flux. The greater currents (and non-total blockade by the specific ASIC1a blocker PcTX) in the top trace perhaps indicates an ASIC1a+2a heteromeric channel population. The upper cell baseline in Figure 22 (read as 0.5959), with the 1st spike (0.7710), an increase of (0.1751) equating to a 29% increase in calcium. A minor spike occurred during the PcTx application, indicating that a small population of the channels being assayed for calcium gating were not blocked by this specifically acting pharmacological agent. By the very composition of the neuronal surface, many overlapping populations of channels are involved in the summated assay of this calcium gating activity; the most logical interpretation of this activity spike, however minor, indeed supports the model presented within this dissertation of heteromeric subunit assemblies being the prominent population in the mouse OFB. The upper cell baseline in figure 22 (read as 0.0691), with the 2nd spike (0.8401), an increase of (0.2442) equating to a 41% increase in calcium. The lower cell baseline in figure 22 (read as (0.3561), 1st Spike (0.4389), an increase of (0.0828) equating to a 23% increase in calcium. The lower cell baseline in figure 22 (read as (0.4110), 2nd Spike (0.4972), an increase of (0.1411) equating to a 20.9% increase.

To this point, the data were clear evidence for an activation response that promoted calcium gating by both cultured and acutely dissociated mouse OFB neurons.

Calcium gating is not ubiquitous in the mouse OFB cellular population

Figure 23: Calcium Imaging of OFB Neuron & non-Ca^{+2} gating cell

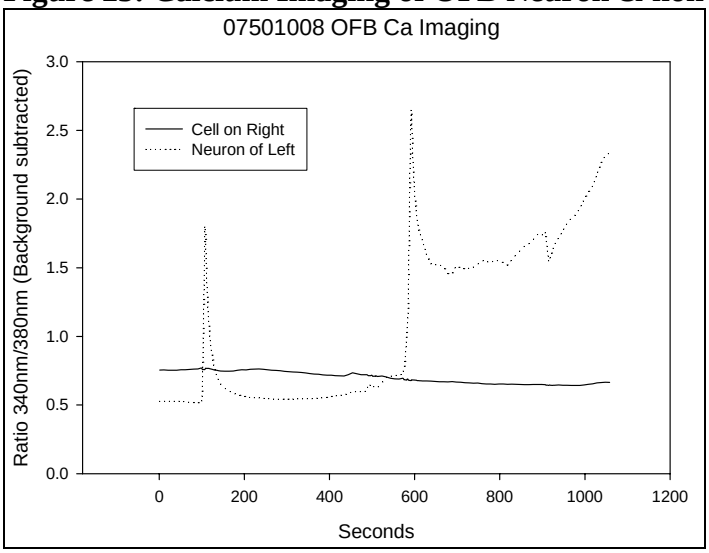

/ *A *B *C /

OFB Calcium Imaging of OFB Neuron & non-Ca^{+2} gating cell gating cell is shown during pH activation; the colormetric ratio of calcium labeled dye versus time.

Visually presented in figure 24, the cell on the left is a neuron gating calcium (Fura-2) and the cell on the right is clearly capable of absorbing the calcium labeled dye, but shows no net movement of calcium during the pH applications, indicating a lack of pH activation of calcium gating, thereby ruling out the presence of ASIC proteins. The ratio imaging process clearly shows in figure 31that the right hand cell is not activated. Depiction markers *A, *B, and *C correspond to the cellular colorimetric dye images in figures 25 and 26 below.

Neuronal populations thus express differing ASIC isoform populations that correlate to direct changes in mouse OFB tissue biophysical functions. Mouse OFB cellular populations also clearly contain cells that do not contain ASIC proteins, as shown in figure 24.

Figure 24: OFB Neuron (*B) with non-calcium gating cell

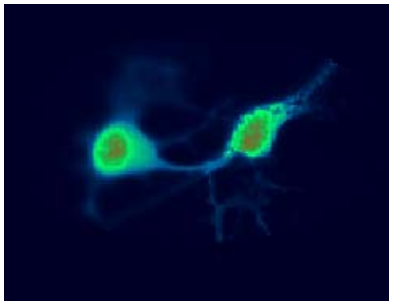

OFB Neuron (*B) with non-calcium gating cell: OFB Neuron (*B) on the left with non-calcium gating cell on the right; both contain dye-labeled calcium ions, only the left hand cell actively gates calcium. Note: this photo equals (*B) above.

Figure 24, showing the so-called "raw" emission only, shows that the cell whose trace is shown as unresponsive (*B) in figure 23, was in fact a healthy cell with an intact membrane and was fully capable of being loaded with Fura-2 dye.

Figure 25: OFB Neuron (*A & *C) with non-Ca^{+2} gating cell

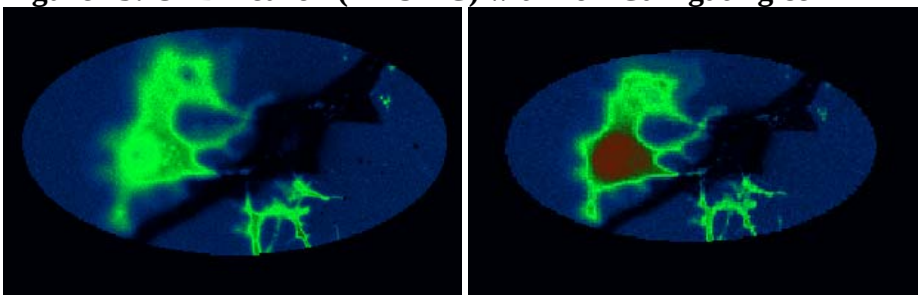

OFB Neuron (*A & *C) with non-calcium gating cell (ratio) clearly illustrates calcium gating being conducted by the left hand cell while to right does not.
Note: equals (*A) above. Note: equals (*C) above.

Calcium imaging was effectively combined with the pharmacological application of agents specifically used to elucidate the isoform composition of the ASIC population in the mouse OFB.

Figure 26: OFB Calcium Imaging w/Amiloride blockade (A-F)

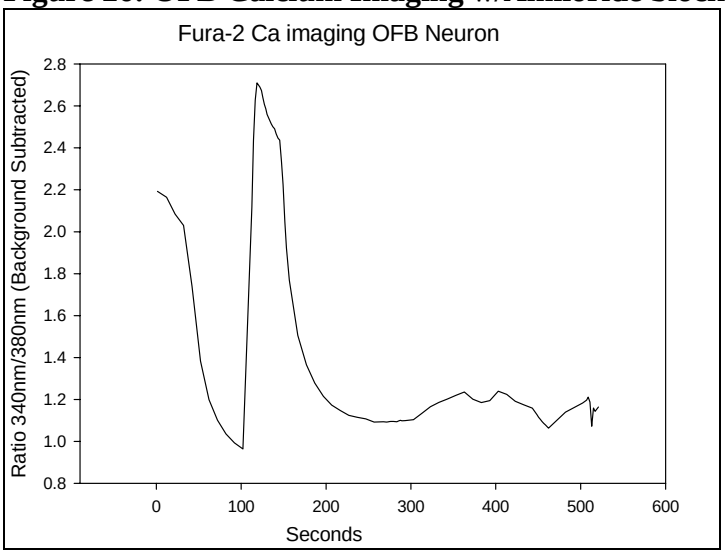

/*A *B *C*D *E *F /

***A (10sec)** ***B (95 sec)** ***C (125 sec)**

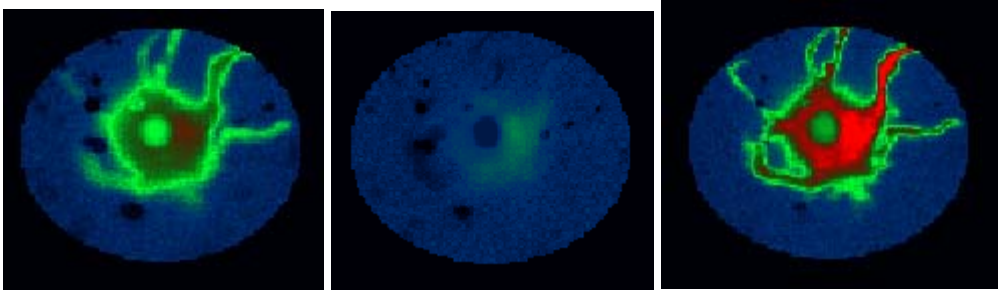

***D (150 sec)** ***E (350 sec)** ***F (480sec)**

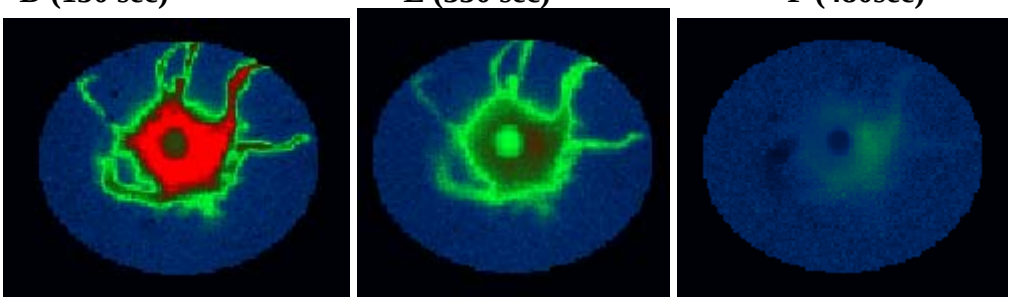

OFB Calcium imaging w/amiloride blockade (A-F) depicts colorimetric ratio cellular images following the chronology of calcium flux shown in the graph. Note the extended duration of this recording. This is a representative example from a large archive of collected data regarding these responses and agent applications to verify ASIC 1a activity in the mouse OFB cellular population.

A verified (KCl assay) OFB neuron undergoing calcium imaging was treated with the general sodium channel blocker amiloride, which effectively blocks ASIC

currents, be they homomeric (1a) or heteromeric (1a+2a) in source. Here in figure 26 amiloride was applied during the 300 to 500 second trials (3 attempts) and no significant ratio increase above 0.1 was detected. Established protocols indicate these results do not represent activation [7,8]. These results qualitatively with color and quantitatively illustrate with numerical ratio values that there is heterogeneity in the mixed population of cells, some of which do not exhibit the gating of dye-labeled calcium ions.

ASIC protein presence confirmed by Western blot technique

Immunodetection by SDS gel electrophoresis of whole neuron homogenates and western blotting confirmed the presence of ASICs in mouse olfactory bulb tissue as shown in figure 27. Negative controls using zero primary antibody (Sigma) but including the secondary labels, showed zero ASIC labeling. Positive controls of cortical neurons and ASIC1a & 2a transfected chinese hamster ovary (CHO) cells are included in this western blot assay for comparison. For clarity, the gel-ladder molecular weight marker band is not shown, and only the relevant portions of the blot are displayed, as probed by an affinity-purified rabbit polyclonal against ASIC (either 1a or 2a) protein (Chemicon International, Temecula, CA). These preparations and methods were identical to previous studies[47,17]. Over-expression of ASIC protein (~58 kilodalton) is evident in the large bands representing the transfected CHO cells, which is one of several standard cell lines used for transfection and transfer of a specific (protein) function for investigation. The comparison of ASIC1a and 2a expression levels in adult versus embryo tissue (Figure 27) was part of an ongoing study in this laboratory, and though not a focus of this dissertation, the evident difference between adult and embryo seen here could be consistent with developmental changes of ASIC expression.

Figure 27: Western Blot of neuron, OFB, & CHO cell controls

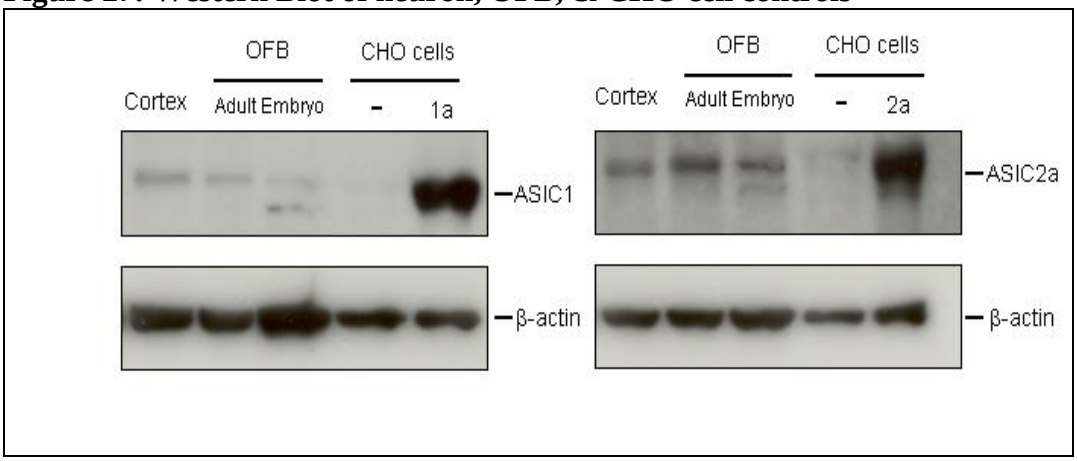

Western Blot of neuron, OFB, & CHO cell controls: Excised gel bands illustrate presence of ASIC protein in mouse cortex, OFB adult and OFB embryo tissues, and (positive control) transfected CHO cells. Beta actin protein was probed as a standard cellular marker as a positive control for the immunostaining technique and the amount of homogenate loaded on a lane.

As the generic antibody recognizes an epitope on the ASIC transmembrane domain region common to both the 1a and 2a isoforms, the illustrated pair of bands in the OFB embryo lane are structural verification of heterogoneitiy in the ASIC subunit population. It is possible that the multiplicity of electrophoretic bands reflects the presence of several gene product versions of these proteins in their native state. It is also possible that the differences in molecular weight represent a cleavage of the protein as part of its post-translational processing.

In short, figure 27 is immunological corroboration of the presence of ASIC in cultured OFB neurons, and the heterogeneity of gel bands is intriguing though not necessarily correlated with the heterogeneity in the ASIC channel activity discovered by the electrophysiological experiments in this dissertation.

Tissue level organization of ASICs in the mouse OFB

Immunocytochemistry (ICC) is a powerful molecular labeling technique for loca;izing an antigen in fixed cells. Careful consideration was applied to the timing and chemical treatments of the mouse OFB tissue contained in this dissertation. The technical devices of cold stage mounts and tissue slicing equipment is detailed

herein, (see Materials and Methods) as well as the antibody components of this visually compelling series of ICC images that follow in figures 28 through 30.

The OFB is columnar (barrel) shaped organ, and they anatomically are a paired set per animal. The outlines of these columns of tissue are show increasing in magnification in figures 28 through 30. The image slices seen here correspond to the OFB column location that is approximately half way between the epithelial interface (the tip) at the upper anatomical junction of the nasal cavity and the thicker base where afferent olfactory sensory projections are rooted into the entorhinal cortex (the trunk) deep inside the brain itself.

Nonspecific labeling during implementation of the ICC technique was curtailed by use of blocking buffers specific to the secondary antibodies host-organism. Mixed populations of ASICs are clearly evident in large-scale visualizations. Mixed populations were examined for (ASIC) OFB neurons during ICC imaging. Individual neurons were also confirmed to have both neuronal markers (NeuN and NSE) and ASIC (1a & 2a) labeling in figures 31 and 35, respectively. Over-labeling and saturation of signal did occur in some preparations (data not shown). Dilutions of labeling antibodies were adjusted accordingly.

Figure 28: Anatomical visualization of the OFB I

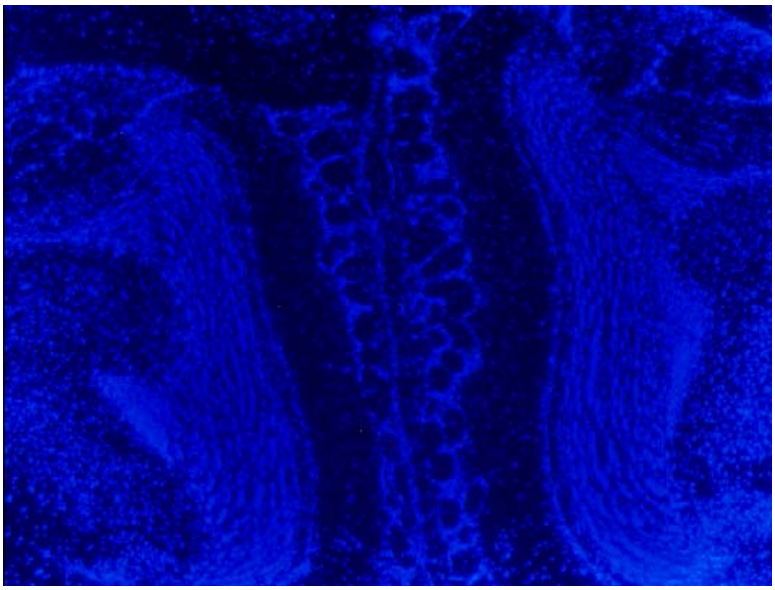

Anatomical visualization of the OFB I: Anatomical visualization of the OFB I: OFB tissue slices imaged using nuclei marker DAPI w/2.5x objective, equivalent to 25x total magnification.

Evident in all ICC tissue images presented herein, the sparse DAPI labeling in the “hole filled” regions around the central trunks of the cylindrical OFB structures allows for several line of interpretation regarding the function of these anatomical regions. This region shows the ‘edge’ of the OFB and the striations of tissue between the two bulbs, the distinct cellular arrangement seen also below. The so-called empty space is actually filled with support cell scaffolding that is shown labeled in later figures.

Figure 29: Anatomical visualization of the OFB II

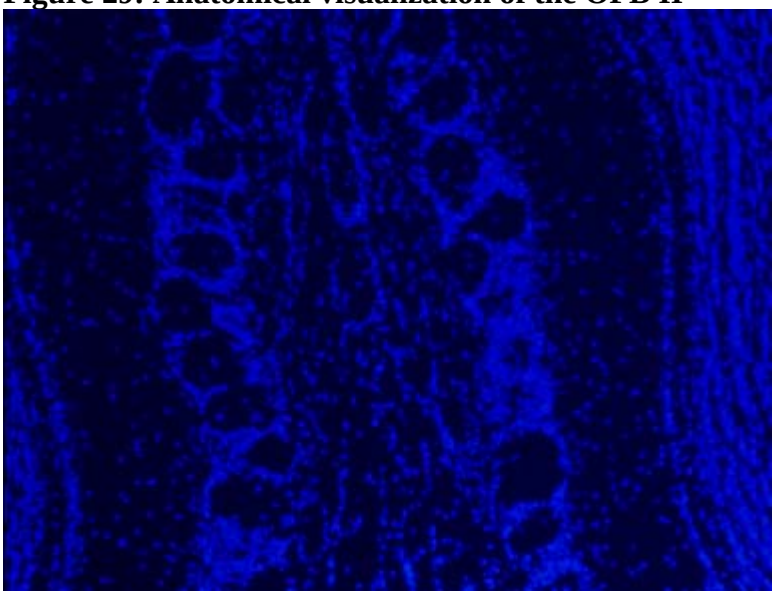

Anatomical visualization of the OFB II: tissue slices imaged via ICC technique labeling cellular nuclei with DAPI (5x objective) at 50x total magnification.

Further magnification of the OFB tissue slice reveals a cellular arrangement, that when overlaid with the ASIC labels, reveals locations for the ASIC containing cell population. The outer sheath of the columnar shaped OFB organ is shown in figure 30 to contain a large number of ASIC labeling cells. The anatomical location of these ASIC cells will be further elaborated upon in the discussion chapter of this dissertation.

Figure 30: Anatomical visualization of the OFB III

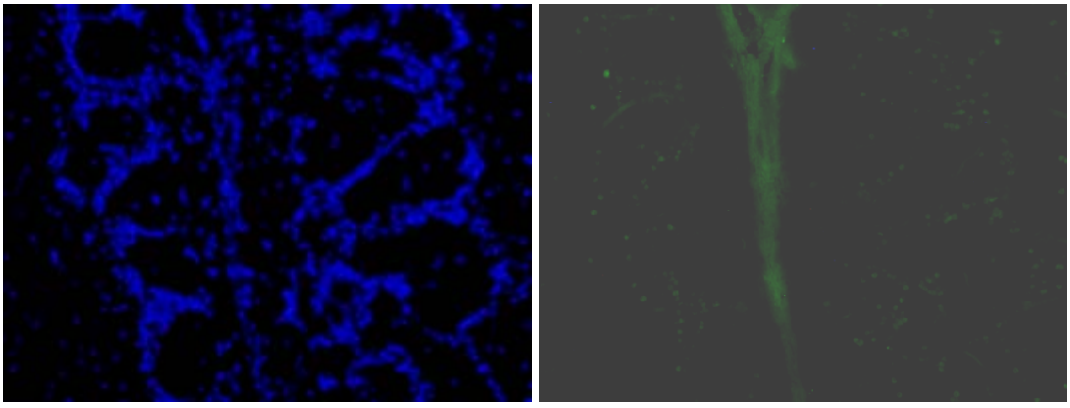

Anatomical visualization of the OFB III: Slices imaged with DAPI and FITC (green, ASIC label) using a 20x objective, equating to 200x total magnification.

ASIC FITC labeling mostly occurs in the lining of the OFB cavity, with sparse labeling in other areas. This supports the theme of ASICs being sensors of neuronal, micro-environmental conditions. Some digital adjustments were used in the ASIC image (right) to better illustrate the distribution of ASICs; they seem interspersed around the apparently vacant regions, which are in reality filled with axonal tracts that terminate both in this OFB region and in the entorhinal cortex of the cerebellum. The ASICs in this preparation are shown positioned in a strategic location for the modulation of normal synaptic current modulation that ravels upstream to the brain itself for further sensory integration. The arrangement of these sensory fields is elaborated upon in the discussion section. The certainty of labeling ASIC containing cells was further strengthened during the course of this dissertation with additional co-localization studies.

Figure 31: ICC of Olfactory Bulb (OFB) neurons (NSE label)

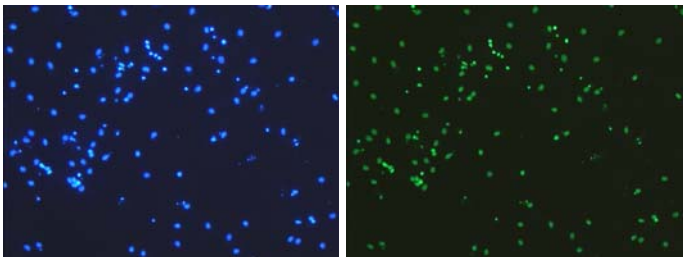

ICC of Olfactory Bulb (OFB) neurons (NSE label): DAPI and FITC labeled NSE (Neuron specific enolase) shown as a positive control of neuronal character for mouse OFB cells obtained from culture.

An additional neuronal marker (neuron-specific enolase) NSE, was used in figure 31 to further support the neuronal character of OFB cells, here shown at 200x total magnification (20x objective). NSE is a nuclei neuronal marker, and the specific identical labeling here demonstrates a sparse population of neurons not yet overgrown with supporting CNS cellular scaffolding.

Figure 32: ICC of Cortical neurons & Astrocytes (native control)

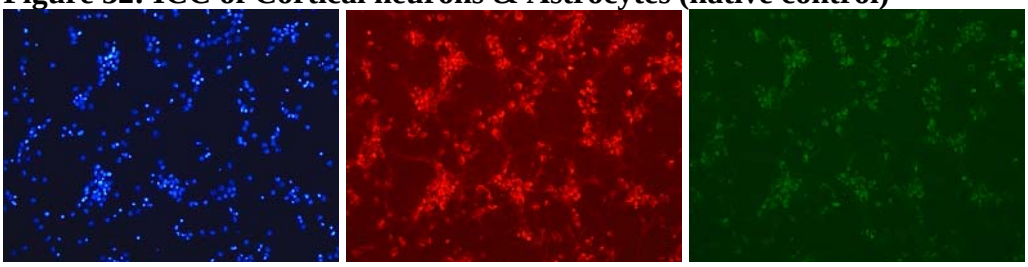

ICC of Cortical neurons & Astrocytes (native control) illustrates a cultured mixed astrocyte neuronal population (positive control) stained with DAPI (blue=nucleus), Cy3 GFAP (red= glial fibrillary acidic protein), and FITC NeuN (green=neuronal specific surface marker), imaged via 200x magnification (20x objective) fluorescence microscope.

Cultured cells were plated and prepared for imaging after 20 days in culture, which as revealed here illustrates the necessity of investigating neurons from short term (12-14 days) in culture. As mentioned previously, overgrowth of non-neuronal population is both native and artifact driven; the nutrient abundance combined with the lack of extracellular scaffolding drives the population dynamics.

Figure 33: ICC of OFB ASIC labeled neurons in mixed population

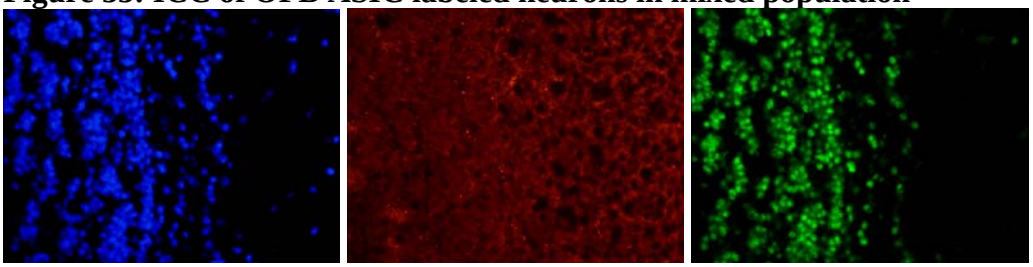

ICC of OFB ASIC labeled neurons in mixed population labeled with DAPI, Cy3 (red, GFAP) and FITC (green, ASIC) imaged using a 20x objective, equating to 200x total magnification.

Note the extensive astrocyte (GFAP) scaffolding, the supporting meshwork; and that non-ASIC labeling (presumably astrocyte) cell structures (shown as blue labeled DAPI) are clearly visible on the right side of the image, away from the ASIC labeled cells.

Figure 34: ICC of OFB neurons (internal negative control)

ICC of OFB neurons (internal negative control: Mouse olfactory bulb neurons underwent ICC protocol with the primary antibody omitted but including the secondary label. This figure therefore images a negative control: DAPI, Cy3, FITC as seen above at 400x total magnification (40x objective).

Visualization of ASICs in tissue level organization

Individual cultured mouse OFB neurons were prepared for ICC visualization and the image in figure 35 is representative of a field of view where some cells are ASIC positive and others are not. Those cells shown in green (FITC-labeled) are ASIC labeled for either ASIC 1a or 2a isoforms, the antibody recognizes a common feature of the ASIC structural amino acid backbone. The entire cellular population is also labeled using the nuclei labeling dye, DAPI. Interestingly, the specific cell types involved (complete characterization of all cell types in the mouse OFB was beyond the scope of this dissertation) did not appear to be as critical a factor as the distribution of ASICs in the tissue level organization. Such anatomically favored distributions of the isoforms independent of cell type is illustrated by the single OFB cells in figure 35.

Figure 35: Individual OFB neurons with FITC secondary to ASIC

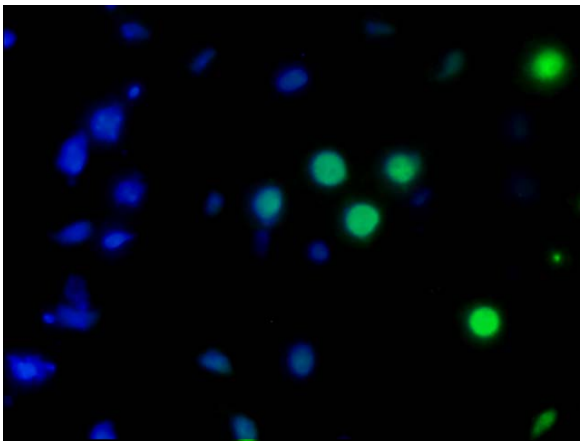

Individual OFB neurons with FITC secondary to ASIC: 400x total magnification fluorescence image with overlay of DAPI and ASIC markers together illuminating individual neurons in culture.

It should be noted that this image was cropped and further reduced by 45% for page formatting. ASIC1a & 2a antibody to ASIC transmembrane domain epitope was used. Note that some (presumably glial) cells are not labeled by (ASIC) FITC, indicating a mixed population. Adjustments made to the image's intensity and opacity parameters better allowed visualization of ASIC labeling in these OFB neurons. Not shown for clarity in figure 35 is the supporting astrocyte scaffolding (GFAP=red).

Figure 36: Closeup of OFB interneuron region

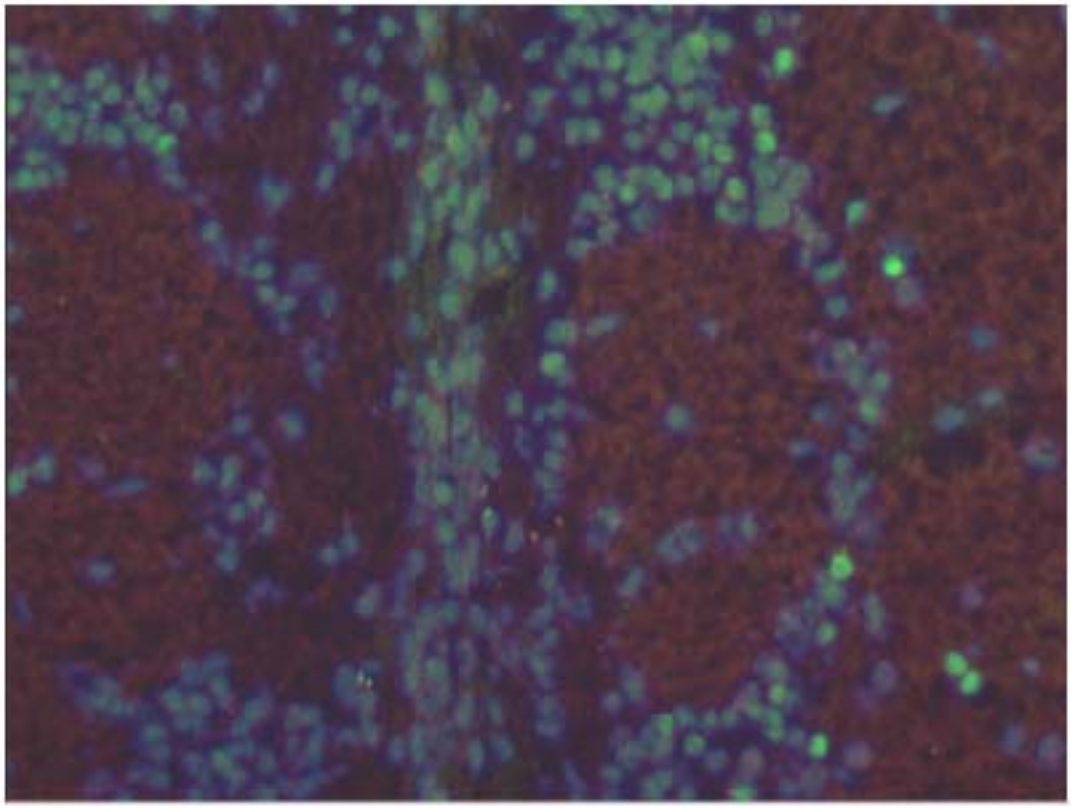

Closeup of OFB interneuron region labeled with DAPI (blue), GFAP (Cy3=red), ASIC (green=FITC), total magnification of 200x.

This image has been cropped, enlarged, and enhanced in a limited fashion to illuminate the colors more clearly. The core of the OFB interneuron region, ASIC labeled (green) neurons surround the (red) GFAP labeled (astrocyte scaffolding), with additional non-ASIC cells labeled by DAPI. The co-localization of green and blue directly indicate ASIC expressing OFB cells. This image was modified for formatting.

Genetic knockout experiments provided verification of ASIC activity

A powerful molecular biological tool for elucidating a specific protein function or ion channel is to remove, or “knockout” the gene encoding that protein. ASIC1a (ASIC) and ASIC2a (ENC1) knockout mice were generated in Dr. Welsh’s laboratory at the University of Iowa and mating pairs were graciously donated to

this laboratory. A gross phenotypic change due to ASIC deficiency has not been discovered in either of these knockout animals. However, a more detailed analysis showed that LTP (long-term potentiation) measured in brain slices is reduced for ASIC1a knockout mice, suggesting an ASIC1 role in synaptic plasticity, learning and memory, while ASIC2a knockout mice showed reduced touch sensation[48],[30].

In this dissertation, ASIC1a knockout animals were used as a source of cultured OFB neurons as a definitive framework to corroborate an ASIC gene product as the origin of the electrophysiological activities assayed. Knockout mice neurons were assayed using identical procedures and reagents described above for wild-type mice.

As shown by figure 37, electrophysiological monitoring of cellular current following reductions in pH from 7.4 to 6.0 did not activate ASICs in knockout cultures of 12 days of age (N=7). The response was essentially a flat line despite a pH drop that activates current in the -2000 picoamp range in wild-type neurons (Figure 37, right).

Next, calcium imaging was conducted to verify ASIC1a participation in calcium entry (Figure 39). Fura-2 fluorescent Ca^{2+}-imaging demonstrated pH reduction from 7.4 to 6.0 did not trigger a detectable increase of $[Ca^{2+}]_e$ in 5 out of 5 neurons. . Knockouts were also prepared for ICC method as above, with zero labeling of ASICs (Figure 40)

Pharmacological assays of knockouts support previous findings

Application of amiloride (30uM, N=5) to knockout mice OFB neurons did not change the baseline current, verifying that this current did not derive from sodium channels, thereby excluding ASICs in a general sense. The specific blockade by PCTX was not effective in preventing inward current flow, indicating ASIC2a subunits were capable of cation flux, albeit not in the same pH sensing range; in 4

out of 5 neurons, lowering pH to 4.0 triggered inward current with an amplitude >500 pA, an overall three-fold suppression. Furthermore, the currents in these neurons display the characteristics of ASIC2a currents, being sensitive to Zn^{2+} potentiation (data not shown) but being insensitive to the physiologically relevant pH change to 6.0.

ASIC1a Knockout shows zero current activation

Figure 37: ASIC1a Knockout current samples

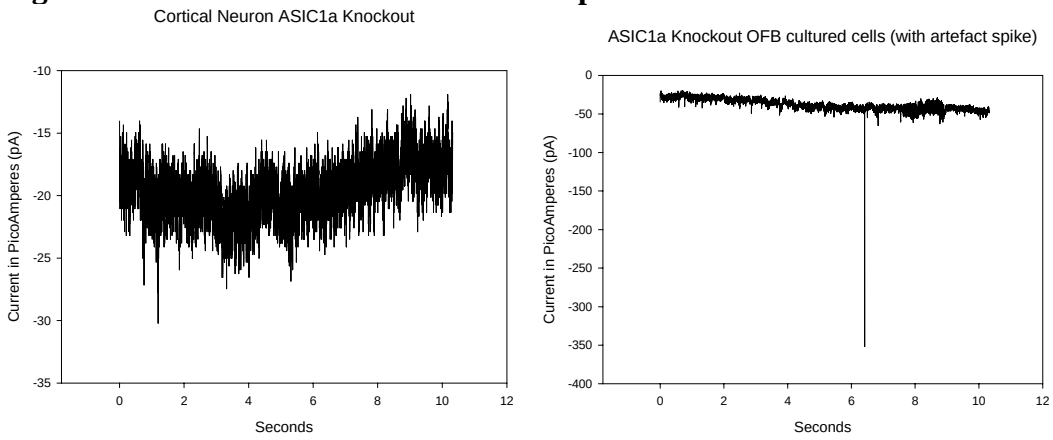

ASIC1a Knockout current samples: Current (pA) versus time showing the differing scales of fluctuation during knockout assays were equivalent to baseline channel activity.

To measure current activation, ASIC1a knockout OFB neurons were electrophysiologically assayed under voltage clamped conditions to measure channel activity. As shown in figure 37, no currents were detected when the pH was lowered from 7.4 to 4.0 were applied at the 1 second marker. Also note how fluctuation of the current by about 20 pA is the wild-type level of fluctuation. To ensure that the knockout mice neurons were viable neurons, they were examined by the standard practices described above, namely currents that did not stabilize were not included in further investigations, and cells were verified as neurons by 50mM KCL application. Note that in these figures, no response is evident even though the Y-axis scale has been blown-up compared to previous figures describing channel currents in wild-type neurons. In these figures, the clarity of these negative findings for the presence of ASIC protein confirmed the viability of

our knockout animal strains in the absence of functional ASIC1a activity, and further supported via corroboration the evidence mounted within this dissertation of the heteromeric population of ASICs in the mouse OFB.

Figure 38: ASIC 1a Knockout comparison to native Cortical Neurons

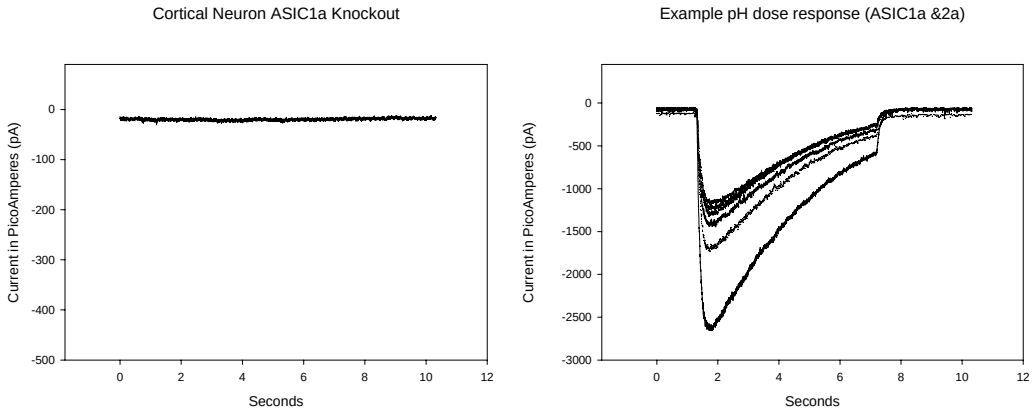

ASIC 1a Knockout comparison to native cortical neurons, Left graph, shows ASIC1a genetic knockout assayed concludes zero ASIC activity (pA). Right graph shows current of native cortical neurons with typical ASIC acid response.

Figure 38 compares the measurement of pH activation of ASIC currents in knockout (left) versus wild-type (right) positive control cells. For clarity, only one sweep is shown on the left, whereas several sweeps, with accompanying rundown of the current response, are shown in the wild-type cortical neurons on the right. The differences in scale of the two graphs shown in figure 46 are noteworthy; the minor, virtually flat fluctuation at an approximately 5-fold more sensitive scale of the ASIC1a knockout sample still indicates no current, ASIC or otherwise, and only residual channel activity upon exposure to pH treatments, which always occurred at the one second marker on the horizontal scale.. Since there was no current at all, this supports the notion that functioning homomeric ASIC2a channels could be completely absent from ASIC1a knockout cells.

Figure 39: Calcium Imaging of ASIC 1a Knockout Mouse OFB cells

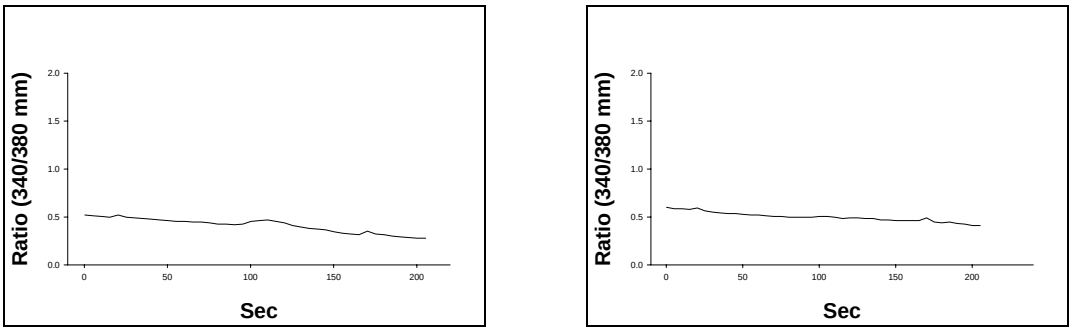

Calcium Imaging of ASIC 1a Knockout Mouse OFB cells: Fura-2 dye colormetric ratio versus time is shown in figure 47, the fluctuating, somewhat horizontal traceline of assayed dye activity. Activation requires a more significant ratio spike, from 1.0 to 2.0.

To assay calcium influx, ASIC1a knockout mouse OFB cultured cells (12days) were prepared for Fura-2 calcium imaging as described previously Result in figure 47 represent several minutes of recording time. All attempts to activate ASIC1a using pH 6.0 were not effective (N=4). The corresponding cellular images (not shown) did not show any changes in the spatial distribution of dye changes.

Figure 40: ICC labeling of ASIC Knockout sample

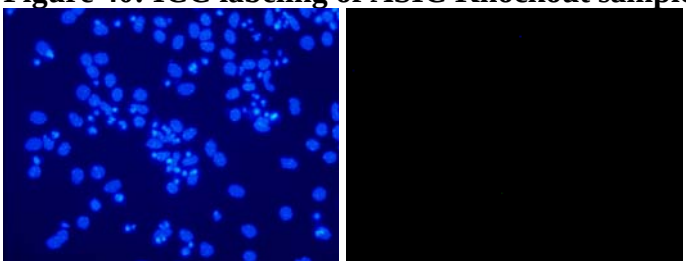

ICC labeling of ASIC Knockout sample: Negative control: of immunocytochemical (ICC) labeling shown as blue illuminated DAPI highlighting the location cellular nuclei, and ASIC (1a or 2a), at 400x magnification (40x objective). Clearly ASIC labeling is lacking.

No ASIC1a immunoreativity was detected when knockout OFB neurons were examined by ICC imaging. representative images of negative results are shown in figure 40 with DAPI, Cy3 (ASIC) labeling of OFB neuronal cultures (N=5). Absence of cellular labeling from the ASIC antibody was structural validation of the null electrophysiology of knockout neurons.

Chapter Five: Discussion

Proteins that sense pathology

A common mechanism for both spreading depression and ischemia would rely on ion channel permeability changes resulting in ion influx of both sodium and calcium[26]. Tissue damage triggered by acidosis, oxygen-glucose deprivation, or other ischemic insults calcium-entry occur via a pathway that is separate and distinct from the glutamate receptor system; a receptor / ion channel that is able to conduct calcium under pathological conditions, the ASICs[27]. The toxicity of intracellular calcium levels are not well understood; apparently there exists a cellular threshold of acceptable or useful calcium concentration, beyond which toxic damage may be unavoidable[28].

Clinical therapies relevant to brain injury are experimentally derived from the molecular utility of their neuro-chemical interaction; the acid sensing ion channel isoform 1a (ASIC 1a) is the most promising target for a potential stroke / brain ischemia treatment because it directly gates and influxes calcium, the primary determinant of the extent of neuronal injury[16],[29],[10],[30].

Confirmation of ASIC 1a involvement in this form of glutamate-independent, acidosis mediated system of ion compensation and reduction of neuronal injury is available from several laboratories[16],[10],[30].

The role of ASICs in brain ischemia is being uncovered incrementally, with new discoveries underscoring this endogenous ion channel/ receptor system as a means to further develop novel therapeutic treatments based on cellular chemistry[27]. The role of mediating calcium entry has been attributed to ASICs for several reasons; first, ASIC knockout mice are impervious to the same level of acidosis-type damage that severely injures their native brethren[27]. Second, transfection of ASIC genes into Chinese hamster ovary cells (CHO cells), or HEK-293 cell line, or even Xenopus oocytes will incorporate the ASIC gene products into the cellular

membranes, and establish the same (ASIC) sensitivity to acidification and oxidative stress, along with the concomitant calcium entry and damage increase[27]. Additionally, ASICs have been demonstrated to gate calcium as confirmed by fura-2 imaging[31].

Mechanism of ASIC sensing

The ASIC permeability of sodium-calcium gating presumably depends critically on the binding of an exterior ligand, most likely in the form of protonated water, known as the hydronium ion (H_3O^+), or perhaps free protons themselves. Presumably the proteinaceous channel must then undergo a change in its conformational structure in response to such changes in acidity. The electrophysiological current traces presented in this dissertation resolve currents at the temporal scale of these structural changes in the channel so that the current directly correlates to channel gating.

Establishment of the mouse OFB as a model system for neuronal study

This dissertation work has succeeded in developing the *in vitro* mouse olfactory bulb neurons as a system for studying ASICs, particularly from the standpoint of asking how combinations of channel isoforms function in living neurons. The power of the system was built, in part, from current knowledge of how to successfully maintain such cells under controlled laboratory conditions, and in part from gaining experience through repeated trials of which conditions and procedures produce success.

It takes a degree of dissection finesse to harvest neuronal cells in good viable yields from olfactory bulb. The precise description of the optimized procedure has therefore been laid out in this work. Further optimization of the system then came from what amounted to a trial-and-error examination of alternative methods of maintaining the cells. Optimally, cells were seeded and grown on both 35mm plastic dishes and 22mm circular glass coverslips for electrophysiology/

immuncytochemistry and calcium imaging respectively. The care of feeding of cells was conducted by an optimized regular schedule, an important methodological adjunct being the periodic examination of cells for viability and activity.

Validation of the mouse OFB system by electrophysiology

The presence and activity of ASICs was functionally measured in the first step of validating the OFB model system. The ultrafine resolution required to assay channel opening and closures is, of course, the forte of the methods of electrophysiology. An applied current essentially “clamps” the membrane, forcing the voltage to remain constant. Any deviation from this “holding potential”, measured in picoamps of membrane current, is directly attributable to the activity of the channel population within the tiny circular section of neuronal membrane being assayed by the electrode’s glass syringe. Both the membrane voltage (number of ions) and the current flow rate in picoamps were assayed repeatedly.

The important outcome of this collective evaluation of the cells by electrophysiology was a verification that the currents and holding potentials observed were fully consistent with those shown previously to be characteristics of acid sensing ion channels in other cellular systems. Hence, as the work proceeded, there was no lingering question as to whether the function under study was ASIC-like in nature. What remained a question, and indeed what erupted as an interesting view of channel function, was the issue of channel heterogeneity, an issue resolved by pharmacology, calcium imaging, and immunodetection as follows.

Pharmacological validation of ASIC heteromeric character

The delivery of extracellular solution washes and specific drug treatments or pH applications were performed by a computer controlled multi-barrel perfusion system, allowing strong fidelity of replication and ultra precise control of the temporal component of (drug) treatment exposure. The well-documented

pharmacological specificity of PcTX's inhibitory action on the ASIC1a isoform was further explored herein to establish the presence of ASIC1a as a subunit contributor to the ASICs being assayed. A series of pharmacological agents (including amiloride, PcTX, zinc and TPEN) were administered during controlled *in vitro* conditions, and the purity of these reagents is without question. While no single agent may fully explain the components of a multi member subunit channel, a corroborative framework was constructed in this dissertation using several drug treatments, in conjunction with pH application responses; the functional overlap of these varied experiments further supported the proposed case of heteromeric ASIC assemblies being the dominant population of said channels.

Validation of ASIC1a activity by calcium gating

The gating of calcium is extremely important for both normal and pathological conditions that effect neurons in the mammalian brain. Imbalance of ion intake and efflux often leads to cellular necrosis, or may alternately initiate apoptotic processes, culminating in both cases with cellular death. The ASIC1a isoform of the channel is responsible for the flow of calcium through the channel, and therefore the presence of ASIC1a in abundance in the OFB model system indicated a cellular population sensitive to acidic microenvironmental changes and that effectively use calcium ions as an external signal regarding the sensing of external pH conditions. Determination of the type of ion passing through the channel was corroborated by cross-comparing the results of electrophysiology and calcium imaging, and was also quantitatively determined by a voltage stepping procedure which ultimately constructed IV curve of current changes versus voltage steps. A subpopulation of cells in evidence in the cultures having no calcium influx proved that heterogeneity in the system also lies at the level of the cell, some of which are missing functional ASICs.

Desensitization studies support heteromeric channel composition

Channel property kinetics requires a brief duration when the channel must remain closed. This desensitized state entails that ligands normally activating the channel would be ignored at the molecular level, as conformational changes may be masking the binding site until the channel recovers. The established recovery duration after ASIC acidic exposure activation is 2 minutes, to allow for maximal responses in the next round of activation. The rapid mechanism of ASIC1 recovery differs from ASIC2, which has a much slower recovery time.

The so-called refractory period following channel activation cannot be avoided. Individual channels must perform this action. However, the entire population of channels may not respond in an identical manner; that is, all channels do not recovery at the same rate. This sub-population of ASIC channels that recovery more quickly may or may not be in the larger population of channels that were activated by the initial acidic exposure.

The normal two-minute recovery period was shortened stepwise to determine the amount of current that is able to ‘penetrate’ the desensitized state. Again it must be emphasized that the entire population of channels (within the patch pipette) is exposed, but not necessarily activated. Current derived from a recovery from desensitization experiment (Figure 16) were normalized to the maximal channel activation current, the percentage of channels available for ion gating at each time interval was determined, and so the current and the population of channels directly correlate, this relationship is valid.

If some channels are not activated in the initial exposure, do they somehow serve as ‘reserve’ sentinels, still on standby to send the alert signal if an additional environmental insult is detected? Does the initial acidic exposure somehow trigger some channels to remain closed, to specifically serve this ‘reserve’ function? Perhaps uncharacterized post-translational modifications allow even further

discrimination in the initial response, providing a subpopulation of channels that are blockaded, but then are essentially primed for activation by the initial exposure, rather than actually being activated. This staggered series of activation profiles is one biological strategy to maintain a continuous sensory apparatus for the sensing of internal pH conditions.

Detection of ASICs in mouse OFB by Western blotting

The detection of ASIC protein isoforms 1a and 2a were conducted in this dissertation using the Western blotting technique. Heterogeneity in ASIC content was evident between the adult and embryonic samples, represented by pairs of gel-bands very similar in molecular weight. This result likely corresponds to the functional heterogeneity of the functioning channel, structurally related to processing of the ASIC protein by proteolytic cleavage or heterogeneity of expressed genes. Transfection and forced over expression of ASICs in the CHO cell system, in addition to oocytes and HEK 293 cells (data not shown) was a system which provided robust cellular positive controls.

Detection of ASICs in mouse OFB by Immunocytochemistry (ICC)

The common epitope of ASICs recognized by the antibody utilized in this dissertation entailed a labeling of both isoforms in the same preparation, thereby excluding the possibility of distinguishing between them their respective expression patterns. However, tissue level organization and single cell labeling of ASIC protein was successful and helped reveal the putative physiological roles of ASICs and its anatomical pattern across the mouse OFB system.

Definitive validation by genetic knockout sample comparisons

The weight of evidence thus far accumulated pointed strongly to ASIC structure and functions. Formal and definitive proof of this assertion was finally obtained by examining cells taken from gene knockout animals lacking the ASIC1a gene. A striking and complete absence of electrophysiological and immunological signals

for all ASICs was the hallmark of the cells from knockout animals. The knockout results then support the hypothesis which states that functional involvement of the ASIC2a isoform requires the presence of ASIC1a. Thus, the measured currents that were qualitatively judged to be an ASIC2a in nature (by PcTX- and zinc-sensitivity) are most probably conducted by heteromeric assemblies involving combinations of ASIC1a and ASIC2a. This result is one of the first to reveal the critical role played by combinations of subunits to produce acid sensitive currents.

New knowledge obtained about ASIC structure and function

This dissertation established an ideal model system of the study of ion channel protein composition in the mammalian brain. More specifically, the olfactory bulb region, composed of several cell types housed in a columnar shaped tissue was determined to contain functional ASIC heteromeric channel assemblies by a variety of corroborative assays; provided by several avenues of experimental evidence, the sheer amount of which is compelling. Only a small portion of representative results are presented herein, to support the stated hypothesis of heteromeric ASICs being the largest population contributor to the mouse olfactory bulb signal routing function. ASIC modulation of and participation in normative neuronal synaptic signaling is becoming more likely with continued investigations.

ASIC heteromeric assemblies provide a more refined version of the ASIC 1a homomeric channel, which conducts calcium in response to reductions in pH in a very straightforward manner. The addition of the ASIC 2a subunit (isoform) to the assembly radically alters the secondary biophysical properties of the channel, and indeed the channel’s role in the nervous system physiology of the organism. Aberrant activity of ASICs may be the root proteinaceous correlate to neuronal pathologies such as stroke, ischemia, epilepsy, and even traumatic brain injury. The further investigation of the ASIC system in mammalian model organisms is encouraged. The fundamental understanding of these functions will be crucial to the full elucidation of ASIC functions in both normal and pathological responses.

Chapter 6: Conclusion

The prominent functional role of calcium in neuronal physiology is an enormous field; specifically for this dissertation, the of calcium gating conducted by the ASIC1a isoform holds functional relevance in several neuronal pathologies, making the study of ASIC heteromeric combinations a vital step toward elucidating the full range of modulation functions performed by ASICs. This dissertation investigated the presence and activity of ASIC isoform heteromeric combinations of the ASIC 1a plus 2a isoforms; the subtle yet revealing biophysical differences incurred through the inclusion of the ASIC 2a subunit and its established ability to alter the so-called secondary biophysical parameters such as recovery from densensitization and refractory period duration. These issues are examined in this work, and validly strong experimental results were obtained during the preparation of this dissertation. However, only a small portion of representative results are presented herein in figures 20 through 25 very much support the ASIC 1a + 2a heteromeric combination as being the dominant protein subunit quanternary amino acid structure, also known as multermericity.

While homomeric ASIC1a channels conduct the majority of current, it was experimentally verified that both the relative isoform contributions and the absolute (total) ASIC amount determined the current amplitude (raw ion flow) and secondary biophysical properties[49],[50],[49]. These ASIC currents and heteromeric currents were verified in all OFB samples presented in this dissertation. Neuronal populations of ASIC channels were found to be heterogeneous in their population-distributions and the percentages of each ASIC isoform forming heterozygous channel combinations was determined; a majority of the measured current was obtained from ASIC1a/2a heteromultimeric channels, the largest population percentage[49]. Heteromeric complexes were determined to be the major component of ASICs in mouse OFB samples presented in this dissertation. Null mice for ASIC1 and ASIC2 were used to determine the biophysical properties that each channel isoform were responsible for[49],[30],[51]. This dissertation utilized this

powerful genetic verification tool as well. The anatomical source of the OFB neurons for studies presented herein is absolutely certain. These biophysical and biochemical characteristics are specific for ASIC proteins, and the validity strength of their presence and activity in the mouse neonatal primary culture and adult acute dissociation cell sources is shown definitively in this dissertation. ASICs form both homomers and heteromers with pH 50 values of 5.8 for ASIC1a homomeric channels and about 5.5 for ASIC 1a+2a heteromeric channels[52]. These values were verified by this dissertation.

ASICs form both homomers and heteromers with pH 50 values of 5.8 for ASIC1 homomeric channels and about 5.5 for ASIC 1a+2a heteromeric channels [124]. Shifts in extracellular pH from 7.4 to 7.0 trigger an inward sodium intake that is sensitive to blockade by amiloride, with a half maximal blockade (IC: 50) at 6.2 microMolar concentration, although significant variation indicated heterogeneity in the ASIC isoforms present in the channels studied[52]. Confirmation of microMolar amiloride effectiveness on mouse OFB ASICs occurred in this dissertation. The known sensing function of ASICs (glucose, redox, divalent cations) combined with verified presence and activity in primary cultured OFB tissue, reinforced with acutely dissociated adult OFB samples, provides rational valid evidence for ASIC protein isoform involvement in OFB functions such as signal modulation and sensory field detection, amplification and discrimination. Tissue level modulation; sensing of environmental contaminants (redox), and pH allows for an ‘early warning system’. Cellular modulation performed by OFB mouse cells is the sensing of pH at the molecular scale, the sensitivity of defining a proper signal from background noise fluctuations; the fundamental property of signal transduction. Empirical conclusion: All experiments indicate ASIC 1a+2a isoform composition as a major contribution to the varied cellular population of both receptors and interneurons in mouse olfactory bulb system.

Heteromeric channels are predominant in single OFB cells

Combinatorial functionality, operating through permutations in the composition of ASICs, allows for new functional boundaries to be explored by the protein and by the neuron, which is a direct expansion of functional survival characteristics. The monitoring of the neuronal microenvironment is crucial

Theoretical conclusion: OFB ASICs participate in interneuron modulation of olfaction signals, the establishment of discriminatory and amplification zones, and possibly as direct environmental sensors within putative receptors in the OFB.

Null conclusions: Full elucidation of each ASIC combination's pharmacological responses was not the purpose of this study. Relevance of this protein in this tissue was not the function of this study. The physiological role of this protein in the animal was not the function of this study.

During the completion of this dissertation, an interesting crystallographic study proposed a channel composition of three subunits. However, no work has ever definitively shown the number of functional ASIC subunits *in vivo*, or examined whether this number might vary; the interchange or removal or addition of subunits is suggested here to correspond with functionally desensitized state, at least under the extreme conditions required for the aforementioned study. This timely coincidence of structural and functional discoveries further illuminate ASICs as an important aspect of neuronal activity.

Reference List

1. Garcia-Anoveros,J., Derfler,B., Neville-Golden,J., Hyman,B.T. & Corey,D.P. BNaC1 and BNaC2 constitute a new family of human neuronal sodium channels related to degenerins and epithelial sodium channels. *Proc. Natl. Acad. Sci. U. S. A* **94**, 1459-1464 (1997).

2. Coric,T., Zhang,P., Todorovic,N. & Canessa,C.M. The extracellular domain determines the kinetics of desensitization in acid-sensitive ion channel 1. *J. Biol. Chem.* **278**, 45240-45247 (2003).

3. Touhara,K. *et al.* Functional identification and reconstitution of an odorant receptor in single olfactory neurons. *Proc. Natl. Acad. Sci. U. S. A.* **96**, 4040-4045 (1999).

4. Oka,Y., Nakamura,A., Watanabe,H. & Touhara,K. An odorant derivative as an antagonist for an olfactory receptor. *Chem. Senses.* **29**, 815-822 (2004).

5. Oka,Y. *et al.* Odorant receptor map in the mouse olfactory bulb: in vivo sensitivity and specificity of receptor-defined glomeruli. *Neuron.* **52**, 857-869 (2006).

6. Zha,X.M., Wemmie,J.A., Green,S.H. & Welsh,M.J. Acid-sensing ion channel 1a is a postsynaptic proton receptor that affects the density of dendritic spines. *Proc. Natl. Acad. Sci. U. S. A.* **103**, 16556-16561 (2006).

7. Alvarez,d.l.R., Canessa,C.M., Fyfe,G.K. & Zhang,P. Structure and regulation of amiloride-sensitive sodium channels. *Annu. Rev. Physiol* **62**, 573-594 (2000).

8. Alvarez,d.l.R. *et al.* Distribution, subcellular localization and ontogeny of ASIC1 in the mammalian central nervous system. *J. Physiol* **546**, 77-87 (2003).

9. Waldmann,R., Champigny,G., Bassilana,F., Heurteaux,C. & Lazdunski,M. A proton-gated cation channel involved in acid-sensing. *Nature* **386**, 173-177 (1997).

10. Zhang,P., Sigworth,F.J. & Canessa,C.M. Gating of acid-sensitive ion channel-1: release of Ca2+ block vs. allosteric mechanism. *J. Gen. Physiol.* **127**, 109-117 (2006).

11. Immke,D.C. & McCleskey,E.W. Protons open acid-sensing ion channels by catalyzing relief of Ca2+ blockade. *Neuron* **37**, 75-84 (2003).

12. Paukert,M., Babini,E., Pusch,M. & Grunder,S. Identification of the Ca2+ blocking site of acid-sensing ion channel (ASIC) 1: implications for channel gating. *J. Gen. Physiol.* **124**, 383-394 (2004).

13. Chen,X., Kalbacher,H. & Grunder,S. The tarantula toxin psalmotoxin 1 inhibits acid-sensing ion channel (ASIC) 1a by increasing its apparent H+ affinity. *J. Gen. Physiol.* **126**, 71-79 (2005).

14. Wang,W.Z. *et al.* Modulation of acid-sensing ion channel currents, acid-induced increase of intracellular Ca2+, and acidosis-mediated neuronal injury by intracellular pH. *J. Biol. Chem.* **281**, 29369-29378 (2006).

15. Askwith,C.C., Wemmie,J.A., Price,M.P., Rokhlina,T. & Welsh,M.J. ASIC2 modulates ASIC1 H+-activated currents in hippocampal neurons. *J. Biol. Chem.* **279**, 18296-18305 (2004).

16. Chu,X.P., Close,N., Saugstad,J.A. & Xiong,Z.G. ASIC1a-specific modulation of acid-sensing ion channels in mouse cortical neurons by redox reagents. *J. Neurosci.* **26**, 5329-5339 (2006).

17. Chu,X.P. *et al.* Subunit-dependent high-affinity zinc inhibition of acid-sensing ion channels. *J. Neurosci.* **24**, 8678-8689 (2004).

18. Molliver,D.C. *et al.* ASIC3, an acid-sensing ion channel, is expressed in metaboreceptive sensory neurons. *Mol. Pain.* **1:35.**, 35 (2005).

19. Ugawa,S. *et al.* Amiloride-insensitive currents of the acid-sensing ion channel-2a (ASIC2a)/ASIC2b heteromeric sour-taste receptor channel. *J. Neurosci.* **23**, 3616-3622 (2003).

20. Shimada,S., Ueda,T., Ishida,Y., Yamamoto,T. & Ugawa,S. Acid-sensing ion channels in taste buds. *Arch. Histol. Cytol.* **69**, 227-231 (2006).

21. Drew,L.J. *et al.* Acid-sensing ion channels ASIC2 and ASIC3 do not contribute to mechanically activated currents in mammalian sensory neurones. *J. Physiol.* **556**, 691-710 (2004).

22. Benson,C.J. *et al.* Heteromultimers of DEG/ENaC subunits form H+-gated channels in mouse sensory neurons. *Proc. Natl. Acad. Sci. U. S. A* **%19;99**, 2338-2343 (2002).

23. Bassilana,F. *et al.* The acid-sensitive ionic channel subunit ASIC and the mammalian degenerin MDEG form a heteromultimeric H+-gated Na+ channel with novel properties. *J. Biol. Chem.* **272**, 28819-28822 (1997).

24. Lingueglia,E. *et al.* A modulatory subunit of acid sensing ion channels in brain and dorsal root ganglion cells. *J. Biol. Chem.* **272**, 29778-29783 (1997).

25. Xiong,Z.G., Chu,X.P. & Simon,R.P. Acid sensing ion channels--novel therapeutic targets for ischemic brain injury. *Front Biosci.* **12:1376-86.**, 1376-1386 (2007).

26. Hansen,A.J. & Zeuthen,T. Extracellular ion concentrations during spreading depression and ischemia in the rat brain cortex. *Acta Physiol. Scand.* **113**, 437-445 (1981).

27. Xiong,Z.G. *et al.* Neuroprotection in ischemia: blocking calcium-permeable Acid-sensing ion channels. *Cell* **118**, 687-698 (2004).

28. Stout,A.K., Raphael,H.M., Kanterewicz,B.I., Klann,E. & Reynolds,I.J. Glutamate-induced neuron death requires mitochondrial calcium uptake. *Nat. Neurosci.* **1**, 366-373 (1998).

29. Escoubas,P. *et al.* Isolation of a tarantula toxin specific for a class of proton-gated Na+ channels. *J. Biol. Chem.* **275**, 25116-25121 (2000).

30. Wemmie,J.A. *et al.* Acid-sensing ion channel 1 is localized in brain regions with high synaptic density and contributes to fear conditioning. *J Neurosci* **23**, 5496-5502 (2003).

31. Duffy,S. & MacVicar,B.A. In vitro ischemia promotes calcium influx and intracellular calcium release in hippocampal astrocytes. *J. Neurosci.* **16**, 71-81 (1996).

32. Tombaugh,G.C. & Sapolsky,R.M. Mild acidosis protects hippocampal neurons from injury induced by oxygen and glucose deprivation. *Brain Res.* **506**, 343-345 (1990).

33. Siesjo,B.K., Katsura,K.I., Kristian,T., Li,P.A. & Siesjo,P. Molecular mechanisms of acidosis-mediated damage. *Acta Neurochir. Suppl. (Wien.)* **66**, 8-14 (1996).

34. Ying,W., Han,S.K., Miller,J.W. & Swanson,R.A. Acidosis potentiates oxidative neuronal death by multiple mechanisms. *J. Neurochem.* **73**, 1549-1556 (1999).

35. Yermolaieva,O., Leonard,A.S., Schnizler,M.K., Abboud,F.M. & Welsh,M.J. Extracellular acidosis increases neuronal cell calcium by activating acid-sensing ion channel 1a. *Proc. Natl. Acad. Sci. U. S. A* **101**, 6752-6757 (2004).

36. Wahlgren,N.G. & Ahmed,N. Neuroprotection in cerebral ischaemia: facts and fancies--the need for new approaches. *Cerebrovasc. Dis.* **17 Suppl 1**, 153-166 (2004).

37. Sun,A. & Cheng,J. Novel targets for therapeutic intervention against ischemic brain injury. *Clin. Neuropharmacol.* **22**, 164-171 (1999).

38. Vornov,J.J., Tasker,R.C. & Coyle,J.T. Delayed protection by MK-801 and tetrodotoxin in a rat organotypic hippocampal culture model of ischemia. *Stroke* **25**, 457-464 (1994).

39. Kristian,T. & Siesjo,B.K. Calcium-related damage in ischemia. *Life Sci.* **59**, 357-367 (1996).

40. Love,S. Oxidative stress in brain ischemia. *Brain Pathol.* **9**, 119-131 (1999).

41. Shamloo,M. & Wieloch,T. Changes in protein tyrosine phosphorylation in the rat brain after cerebral ischemia in a model of ischemic tolerance. *J. Cereb. Blood Flow Metab.* **19**, 173-183 (1999).

42. Stenzel-Poore,M.P. *et al.* Effect of ischaemic preconditioning on genomic response to cerebral ischaemia: similarity to neuroprotective strategies in hibernation and hypoxia-tolerant states. *Lancet.* **362**, 1028-1037 (2003).

43. Sweeney,M.I., Yager,J.Y., Walz,W. & Juurlink,B.H. Cellular mechanisms involved in brain ischemia. *Can. J. Physiol. Pharmacol.* **73**, 1525-1535 (1995).

44. Iadecola,C. Bright and dark sides of nitric oxide in ischemic brain injury. *Trends. Neurosci.* **20**, 132-139 (1997).

45. Xiong,Z.G., Chu,X.P. & Simon,R.P. Ca2+ -permeable acid-sensing ion channels and ischemic brain injury. *J. Membr. Biol.* **209**, 59-68 (2006).

46. Chu,X.P. *et al.* Acidosis decreases low Ca(2+)-induced neuronal excitation by inhibiting the activity of calcium-sensing cation channels in cultured mouse hippocampal neurons. *J Physiol* **550**, 385-399 (2003).

47. Chu,X.P., Close,N., Saugstad,J.A., Simon,R.P. & Xiong,Z.-G. Redox modulation of acid-sensing ion channels. *Soc Neurosci Abstr* **30**, 845.9 (2004).

48. Wemmie,J.A. *et al.* The acid-activated ion channel ASIC contributes to synaptic plasticity, learning, and memory. *Neuron.* **34**, 463-477 (2002).

49. Askwith,C.C., Wemmie,J.A., Price,M.P., Rokhlina,T. & Welsh,M.J. Acid-sensing ion channel 2 (ASIC2) modulates ASIC1 H+-activated currents in hippocampal neurons. *J. Biol. Chem.* **279**, 18296-18305 (2004).

50. Hesselager,M., Timmermann,D.B. & Ahring,P.K. pH Dependency and desensitization kinetics of heterologously expressed combinations of acid-sensing ion channel subunits. *J. Biol. Chem.* **%19;279**, 11006-11015 (2004).

51. Roza,C. *et al.* Knockout of the ASIC2 channel in mice does not impair cutaneous mechanosensation, visceral mechanonociception and hearing. *J. Physiol.* **558**, 659-669 (2004).

52. Varming,T. Proton-gated ion channels in cultured mouse cortical neurons. *Neuropharmacology* **38**, 1875-1881 (1999).